Reviews

Vibrational spectra and structural features of noble gas fluorides in cryogenic and nonaqueous solutions

Sh. Sh. Nabiev

Russian Scientific Center "Kurchatov Institute",
1 pl. I. V. Kurchatova, 123182 Moscow, Russian Federation.
Fax: +7 (095) 194 1994

Data on the vibrational spectra of noble gas fluorides in the gas phase and in cryogenic and nonaqueous solutions are considered in detail. Based on analysis of the IR spectra of xenon fluorides dissolved in liquid Kr and Xe, it is concluded that the XeF_6 molecule possesses the geometry of a distorted octahedron with C_{3v} symmetry. The contours of spectral lines of totally symmetric stretching modes in the Raman spectra of noble gas fluorides in nonaqueous solutions are considered; the mechanisms of formation contours of these lines, the dynamic parameters of XeF_n (n = 2, 4, 6) and KrF_2, and the characteristic times of intramolecular rearrangements in the nonrigid XeF_6 molecule are analyzed. It is concluded that in the XeF_2—HF and XeF_6—HF systems, a number of associates and ionic clusters are formed due to the donor—acceptor interaction of the Lewis bases and acids.

Key words: noble gas fluorides, IR spectrum, Raman spectrum, frequency of bond vibration, cryogenic solution, spectral line contour, structural nonrigidity, intramolecular rearrangement, correlation function, vibrational and rotational relaxation.

Introduction

Krypton and xenon fluorides (KrF_2 and XeF_n, n = 2, 4, 6)[1] are widely used as fluorinating reagents in low-temperature inorganic syntheses[2] and in the synthesis of fluoroaromatic, fluoroaliphatic, and heteroorganic (S, Si, P, Se) compounds.[3] Noble gas fluorides are also used for chemical smoothing of semiconductor crystals of Ge, Si, GaP, AsSi, AsGa, and InSb and their oxides, for ion plasma etching of Si, SiO_2, Si_3N_4, *etc.*, and also as the sources of fluorine for high-energy chemical and excimer lasers, components of cathode materials of chemical cells, *etc.*[4,5] Finally, in recent years, extrapure Xe fluorides have been used to prepare high-purity fluorides and to purify fluorides from traces of oxygen and water. For example, these compounds are used to prepare alkali, alkaline earth, and rare earth metal fluorides and Zr and Hf fluorides for optical materials in fiber optics; Re, W, Mo, and Ta fluorides for obtaining thermally stable coatings with impurities of transition metals at the level of 10^{-6} % (w/w).[6]

Study of the properties of noble gas fluorides, most of all their behavior in nonaqueous solvents, made it possible to develop and refine some aspects of the chemistry of inorganic fluorides, the chemistry of nonaqueous media, and the theory of reactivity and complex formation.[2,7] Nonaqueous solutions of Xe fluorides are efficient oxidants ($\Delta G°_{298}(XeF_2)$ = −17.5±2.0 kcal mol^{-1}, $\Delta G°_{298}(XeF_4)$ = −31.4±2.5 kcal mol^{-1}, $\Delta G°_{298}(XeF_6)$ = −38.5±2.5 kcal mol^{-1}, $D°_{298}[XeF_n$ (n = 2, 4, 6)] ≈ −30.0 kcal mol^{-1}; this is due to the low energy of the Xe—F bond, which is comparable to the bond energies in chlorine trifluoride and chlorine pentafluoride[1,8] and is much smaller than those in other inorganic fluorides.

Translated from *Izvestiya Akademii Nauk. Seriya Khimicheskaya,* No. 4, pp. 560—582, April, 1998.

1066-5285/98/4704-0535 $20.00

In recent years, along with xenon fluorides, krypton difluoride has also been actively used as a carrier of F atoms; in fact, the positive standard energy of formation ($\Delta G°_{298}(KrF_2)$ = 22.1±1.5 kcal mol^{-1}) and the low dissociation energy ($D°_{298}(KrF_2)$ = 23.4 kcal mol^{-1}) of KrF_2 point to its extremely high oxidative capacity, which is only slightly lower than that of atomic fluorine ($2\Delta G°_{298}(F)$ = 28 kcal at.$^{-1}$).

Meanwhile, the chemical properties of the noble gas fluorides are markedly dissimilar, especially in nonaqueous solutions.[1] Studies of xenon and krypton fluorides in nonaqueous solutions revealed a series of unique properties of noble gas fluorides and, in turn, resulted in the development of new methods for the synthesis of fluorides and in the discovery of new Kr^{II}, Xe^{II}, Xe^{IV}, and Xe^{VI} complexes.

Vibrational spectroscopy is one of the most useful techniques for investigation of the structure and reactivity of noble gas fluorides. By now, vast experimental material on the vibrational spectra of gaseous, solid, and molten inorganic chlorides, bromides, and iodides of Group I—VII elements has been accumulated.[9—11] Study of the spectra of most of the polyatomic fluorine derivatives, especially, Xe and Kr fluorides, both in the gas phase and condensed state, including their solutions in nonaqueous solvents, is associated with severe methodical and experimental difficulties caused by the high toxicity and reactivity of these compounds. Therefore, the structural features of Kr and Xe fluorides and their complexes are usually studied under nonequilibrium conditions, *viz.*, for molecules isolated in low-temperature matrices of inert gases.[12]

In the present work, exhaustive spectroscopic information on noble gas fluorides was obtained by IR cryospectroscopy and Raman spectroscopy of nonaqueous solutions. Combination of these methods made it possible to study the vibrational spectra of Xe and Kr fluorides over a fairly broad range of frequencies under conditions of minimized interaction with the environment and also to obtain information on the perturbation of various types of molecular motion and on the dynamic characteristics of molecules.

Main spectroscopic procedures

Basic principles of IR cryospectroscopy

The low-temperature IR absorption spectra of solutions in liquefied gases provide a lot of information about the molecules studied.[13,14] The relevant experimental instrumentation, which has been developed since the early 70s, is referred to as "cryospectroscopy".[15] The use of liquid noble gases, which are highly inert and transparent in the range from the vacuum ultraviolet frequencies to the radio frequencies, and liquid oxygen and nitrogen, which exhibit absorption bands in the medium IR region (~1550 cm^{-1} for liquid O_2 and ~2350 cm^{-1} for liquid N_2), as solvents substantially increases the accuracy of determination of vibration frequencies due to the elimination of the bands for "hot" transitions, collapse of the rotational structure, and, consequently, a decrease in the overlap of spectral bands. For instance, the population of the lowest vibrational level of the SF_6 molecule in liquid argon (T = 90±2 K) amounts to ~1%, while for PH_3 molecule, this value is $1.5 \cdot 10^{-5}$%. As a consequence, the vibration-rotational bands degenerate into narrow spectral lines with half-widths Γ = 0.3—6 cm^{-1}. The cryospectroscopic method, whose sensitivity reaches 10^{-10} mole fractions and is practically limited only by the transparency of the solution in the spectral range of interest,[15—19] is used to study volatile compounds that are unstable at room temperature and also highly chemically reactive and toxic compounds.[19—24] The vibrational spectra of molecules in a cryogenic solution make it possible to identify structural fragments and to determine the stoichiometry, symmetry, and geometric parameters of a molecule.[15,25,26] In addition, analysis of the shapes, widths, and shifts of vibration bands provides information on the characteristic features of various types of thermal motion of molecules.[15,27,28] This also enables the detection of weak intermolecular interactions that are not manifested at ambient temperature and investigation of complex formation processes.[15,25,29—33]

Spectroscopy of cryogenic solutions bears a resemblance to the known method of low-temperature matrix isolation.[34—36] However, the use of the matrix method involves the following problems:

1. The matrix isolation method is virtually inapplicable to the investigation of compound bands or overtones ($v \geq 3$) having low intensities in the IR spectra; this is due to the difficulties in the preparation of thick samples and to the scattering of the incident IR radiation by the matrices.

2. The IR spectra of matrix-isolated molecules often exhibit split vibration bands resulting from dissimilar arrangements of molecules between densely packed atoms (molecules) of the crystal lattice of a matrix; in some cases, it is impossible to distinguish the matrix splitting from spectroscopic effects related to physicochemical properties of the molecules studied.

3. Low-temperature matrices are normally nonequilibrium systems, and this precludes investigation of thermodynamic characteristics of some physicochemical processes occurring at low temperatures.

4. The matrix isolation method cannot be used to determine the integral absorption coefficients for the vibration bands of the molecular systems studied.

Among the cryogenic solvents currently used in molecular spectroscopy, liquefied argon and oxygen are the most inert solvents causing the least perturbations of the spectra of dissolved substances. The vibrational spectra of molecules in liquid argon (LAr) and oxygen (LO_2) are fairly close to the spectra of free molecules.[13,15] In liquid krypton (LKr) and xenon (LXe), which are also inert solvents, the spectral effects caused by intermo-

lecular interactions are markedly stronger; however, these solvents are often used, because their dissolving capacities are higher than those of LAr and LO_2.

Determination of the solubility of molecules in cryogenic solutions

The IR-spectroscopic procedure for determining the solubility of compounds in low-temperature solutions is based on the Bouguer—Beer law:[37]

$$x_2 = cV_mB/(N_AlA), \quad (1)$$

where x_2 is the concentration of a solute (in mole fractions), N_A is the Avogadro number (mol^{-1}), V_m is the molar volume ($cm^3\ mol^{-1}$) of the solution, which is equal to the molar volume of the solvent for highly dilute solutions, c is the velocity of light ($cm\ s^{-1}$), l is the optical path length (cm), A is the integral absorption coefficient of the band (cm^2 molec.$^{-1}$ s^{-1}), and B is the integral intensity of the analytical band (cm^{-1}) defined as

$$B = \int_{-\infty}^{+\infty} \ln[I_0(\omega)/I(\omega)]d\omega = \int_{-\infty}^{+\infty} D(\omega)d\omega. \quad (2)$$

Here $I_0(\omega)$ and $I(\omega)$ are the intensities of the incident luminuous flux and that transmitted through the sample, respectively, ω is frequency, and $D(\omega)$ is optical density.

The integral absorption coefficient can be found from the expression

$$A = \frac{c}{Nl}\int_{-\infty}^{+\infty} D(\omega)d\omega, \quad (3)$$

where N is the concentration of the substance.

In practice, the solubility of compounds under analysis in a liquefied noble gas is determined in the following way.[38] First, the A values for the analytical bands of fluoride at various concentrations of a cryogenic solution were measured, and then the B value for a saturated cryogenic solution was found. The x_2 value was calculated from formula (3).

The resulting integral absorption coefficients were recalculated for free molecules using the following relation[13]

$$A_{gas} = A_{sol}\frac{9n}{(n^2+2)^2} = K(n)A_{sol}, \quad (4)$$

where n is the refractive index of the cryogenic solution. For LAr ($T \approx 90$ K), $n = 1.23$, for LKr ($T \approx 130$ K), $n = 1.29$, and for LXe ($T \approx 180$ K), $n = 1.39$. The correction factor $K(n)$ takes into account a set of items mostly associated with the change in the strength of the field of the incident light wave in the cryogenic solution with respect to that in vacuum.

Basic principles for deriving dynamic information on liquid systems from the Raman spectra

The mechanisms of physicochemical processes in solutions are largely determined by the vibrational and rotational relaxation processes, which are related to the stochastic properties of the medium. It is convenient to study the mechanisms of the vibrational and rotational relaxation of dissolved molecules within the framework of the probability theory using the correlation functions (CF) $G_i(t)$, which characterize quantitatively the time evolution of an ensemble of particles caused by their motion and interaction, *i.e.*, they make it possible to convert the frequency characteristics of a process into temporal characteristics.[39,40] A CF describes the manner in which the probability of finding the system under study in the same state in which it occurred in the initial instant t_0 changes with time:

$$G_i(t) = F_i^*(t_0)F_i(t + t_0). \quad (5)$$

Here $F_i(t_0)$ is a dynamic variable, and the asterisk marks the complex conjugate value. Normalization of CF is accomplished by dividing it into $F_i^2(t_0)$; this yields a normalized correlation function $\hat{G}_i(t)$ with the following properties: at $t = 0$, $\hat{G}_i(t) = 1$ and at $t \to \infty$, $\hat{G}_i(t) = 0$.

The polarizability tensor of a particle occurring in the ensemble can be represented as a power series of the normal coordinate of a jth vibration q_j:[39]

$$\alpha_{nk} = \alpha_{nk}^{(0)} + \sum_j (\partial\alpha_{nk}/\partial q_j)q_j + \ldots \quad (n, k = x, y, z) \quad (6)$$

and resolved into the isotropic

$$\alpha' = \sum_n \alpha_{nn} \quad (7)$$

and anisotropic

$$\alpha''_{nk} = \alpha_{nk} - \alpha'\,\delta_{nk} \quad (8)$$

constituents, where δ_{nk} is the Kronecker delta ($\delta = 1$ at $n = k$, $\delta = 0$ at $n \neq k$). The α' and α''_{nk} values are invariants of the polarizability tensor, *i.e.*, they do not depend on the orientation of the coordinate system with respect to the polarizability ellipsoid. The components of the dipole moment P_n induced by the field of the exciting light wave E_k, depend on the corresponding components of the polarizability tensor and can be written as

$$P_n = \alpha_{nk}E_k. \quad (9)$$

To describe the process of the Raman scattering, the q_j-dependent part of the polarizability tensor α_{nk} is isolated:

$$\alpha_{nk}(q_j) = (\alpha'\delta_{nk} + \alpha''_{nk})q_j. \quad (10)$$

The term $\alpha'\delta_{nk}q_j$ in relation (10) forms the isotropic constituent of the Raman scattering, *i.e.*, it characterizes the spherically symmetrical part of the scattered light. In addition, α' is invariant with respect to the molecular rotation, and it is the only value containing a linear combination of the main polarizability values. The term $\alpha''_{nk}q_j$ forms the anisotropic constituent of the Raman scattering. The time dependence of $\alpha_{nk}(q_j)$ is manifested as the time variation of either the components of the polarizability tensor or the normal coordinate of the vibration. The former case implies orientational relaxation associated with reorientation of the particle, because only anisotropic constituents of the polarizability tensor are sensitive to rotations of the particle. In the latter case, a number of phenomena denoted by the term "vibrational relaxation" occur; adiabatic interactions between particles involving no energy exchange can be put into this category. These interactions can result in shifts of vibration levels or in the change of the vibration phase. Nonadiabatic interactions between the particles are accompanied by exchange or scattering of the vibration energy. In this case, the vibration quanta can be either transferred without changes from a vibration level of one particle to the identical level of another particle (V—V relaxation) or transformed into other (vibration, rotation, forward) degrees of freedom of the system (V—V′, V—R, and V—T).[41]

To calculate the intensity of the emission of the isotropic and anisotropic Raman constituents, one needs to know invariants (7) and (8), which can be found by determining the matrix elements

$$\langle v|\alpha|v'\rangle = \int q_j^*\alpha(q_j)q_j dq. \qquad (11)$$

With allowance for relation (11) for the isotropic Raman scattering constituent, the intensity of the scattered light is expressed as follows:

$$I_{is}(\nu) \approx \int_{-\infty}^{+\infty} \overline{q_j^*(t_0)q_j(t)} \exp\{-2\pi ic\nu t\}dt. \qquad (12)$$

Expression (12) provides information only on the vibrational relaxation of an jth vibration of the particle. For the anisotropic constituent of the Raman scattering, the intensity of the scattered light is found as follows:

$$I_{anis}(\nu) \approx \int_{-\infty}^{+\infty} \overline{K[\alpha''^*(t_0)\alpha''(t)]}\ \overline{q_j^*(t_0)q_j(t)} \exp\{-2\pi ic\nu t\}dt. \qquad (13)$$

Here K is the spur of matrix α''.

The orientational relaxation, described by the first factor in the integrated expression in formula (13), and the vibrational relaxation are normally independent of each other. Therefore, they can be averaged separately.

In practice, CFs are determined as Fourier transforms of the isotropic (I_{is}) and anisotropic (I_{anis}) components of the Raman spectrum. Since the processes of orientational and vibrational relaxation are the main mechanisms of the Raman line broadening in the systems under consideration, below we will speak of the rotational and vibrational correlation functions corresponding to these processes. Fourier transform of the isotropic constituent yields directly the vibrational CF ($G_V(t)$), whereas the same transformation of the anisotropic substituent leads to the product of vibrational and rotational ($G_R(t)$) correlation functions:

$$G_V(t) = \int \hat{I}_{is}(\nu) \exp\{-2\pi ic\nu t\}d\nu, \qquad (14)$$

$$G_R(t)G_V(t) = \int \hat{I}_{anis}(\nu) \exp\{-2\pi ic\nu t\}d\nu. \qquad (15)$$

Here t is time, and $\hat{I}$ are intensities normalized in the following way:

$$\int_{-\infty}^{\infty} \hat{I}(\nu)d\nu = 1. \qquad (16)$$

The method for determining the intensities $I_{is}(\nu)$ and $I_{anis}(\nu)$ is based on polarization measurements, which make it possible to obtain two spectra designated as $I_{\parallel}$ and $I_{\perp}$. The intensities of the isotropic and anisotropic components of the Raman line are related to the intensities of the polarized ($I_{\parallel}$) and depolarized ($I_{\perp}$) components of the spectrum by the following expressions:

$$I_{anis}(\nu) = I_{\perp}(\nu), \qquad (17)$$

$$I_{is}(\nu) = I_{\parallel}(\nu) - (4/3)I_{\perp}(\nu). \qquad (18)$$

Yet another characteristic of the processes occurring in these systems is correlation time defined in the following way

$$\tau = \int_0^{\infty} G(t)dt. \qquad (19)$$

Unlike the CF, the correlation time is an integrated characteristic of the processes, and the τ^{-1} value is the rate of disordering of the system.

The vibrational relaxation in liquid solutions is caused mostly by violation of the vibration phase (vibrational dephasing). In this case, the stochastic perturbation of the vibration phase can be characterized by a vibrational correlation function of the following form:[40]

$$G_V(t) = \exp\{-M_2\tau_v[\tau_v(e^{-t/\tau_v} - 1) + t]\}, \qquad (20)$$

where M_2 is the second moment of the isotropic constituent of the Raman line, and τ_v is a temporal characteristic of the phase perturbation.

Depending on the magnitude of the product $\sqrt{M_2}\tau_v = \xi$, two extreme types of the time dependence of the correlation function can be distiguished.

1. $\xi >> 1$. Then $G_V(t)$ has a Gaussian form

$$G_V(t) = \exp\{-\pi t^2/4\tau_V^2\}, \qquad (21)$$

where τ_V is the time of vibrational relaxation.

This is the case of so-called nonuniform line broadening or slow modulation. The average squared frequency fluctuation is much larger than τ_v^{-1}, and at

times of ~1 ps (the order of vibrational relaxation times), the system can be considered to be static. In this case, broadening of the Raman line is caused by the statistical nonuniformity of the distribution of neighboring particles due to slow fluctuations of interparticle distances.

2. $\xi << 1$. Then $G_V(t)$ is exponential.

$$G_V(t) = \exp\{-t/\tau_V\} \quad (22)$$

This is the case of uniform line broadening or fast modulation. The Raman line is broadened as a result of movement of the surrounding particles.

The rotational (orientational) relaxation results from the hindered character of the particle rotation, which is due to its collisions with surrounding molecules. If the change of the orientation of a molecule over time τ is characterized by the angle of rotation of its molecular axes θ, two extreme mechanisms of rotational motion, characterized by different periods during which the molecule is at rest τ_S and in motion τ_F, can be distinguished.[41,42] In one of these cases, reorientation is regarded as rotational diffusion: rotation of a particle through angle θ consists of a large number of noncorrelated steps; each of the steps corresponds to the rotation of the particle through angle ε, and in this case, $\tau_S << \tau_F$. According to the second mechanism, the rotation through the angle θ occurs as a single step, *i.e.*, $\varepsilon = \theta$ and $\tau_S >> \tau_F$. In both cases, no limitations on the rotation angles are imposed.

The process of free diffusion[43] in which a particle rotates as a free rotator characterized by a proper angular momentum J, whose magnitude can change upon collisions occurring with frequency τ_j, can be described in terms of the former mechanism. Two limiting cases can be distinguished: in the J-diffusion limit, both the magnitude and the direction of the angular momentum change, while in the M-diffusion limit, only the direction of J changes.

If the orientational correlation function for the case of rotational diffusion has the simple exponential form[44]

$$G_{RD}(t) = \exp\{-t/\tau_R\}, \quad (23)$$

where τ_R is the rotational relaxation time, then the expressions for the CF obtained in terms of the free diffusion model are fairly complex recurrent equations[45] depending on the type of symmetry of the molecule. At relatively small τ values, the following relations are valid:[46]

$$\tau_j = I/(6k_BT\tau_R) \text{ (J-diffusion)}, \quad (24)$$

$$\tau_j = I/(2k_BT\tau_R) \text{ (M-diffusion)}, \quad (25)$$

where I is the moment of inertia of the molecule, k_B is the Boltzmann constant, and T is temperature.

At short rotation times ($\leq 10^{-13}$ s), a particle normally rotates as a free rotator, and its motion can be described by a correlation function of the following form[40]

$$G_{FR}(t) = \exp(-3k_BT^2/I). \quad (26)$$

As the rotation time increases, the particle experiences increasing perturbation due to interaction with the environment, and the correlation function starts to transform into an exponential form, which corresponds to switching to the rotational diffusion regime.

The known τ_j makes it possible to estimate the angle of rotation ε at the first step of diffusion, proceeding from the assumption that before a collision, the molecule rotates as a free rotator with angular velocity $w = \sqrt{k_BT/I}$:

$$\varepsilon = \tau_j \cdot w = \tau_j\sqrt{k_BT/I}. \quad (27)$$

Currently CFs are found using the following main procedures:[39,40,47]

1. Fourier transform of the Raman line contours found experimentally (the discrete Fourier transform).

2. Simulation of the Raman line contours by an analytical function and subsequent application of the Fourier transform.

3. The method of moments in which the corresponding moments are found by approximation procedures.

To find CFs, we used the first and the second techniques; in the latter case, it was assumed that the profile of the Raman line can be described by a dispersion curve. This gave the following equations for the vibrational and rotational CF:[47–49]

$$G_V(t) = \frac{1}{1-4b/3}\exp(-\pi c\gamma_\parallel t) - \frac{4}{3}\cdot\frac{b}{1-4b/3}\exp(-\pi c\gamma_\perp t), \quad (28)$$

$$G_R(t) = \exp\{-\pi c\gamma_\perp t\}/G_V(t), \quad (29)$$

where $\gamma_\parallel$ and $\gamma_\perp$ are the half-widths of the polarized and depolarized lines, respectively, and b is the ratio of the intensities of the depolarized and polarized constituents of the Raman lines determined at the maximum. The integration of Eqs. (28) and (29) with respect to time gives the following expressions for the vibrational and rotational relaxation times:[47,48,50]

$$\tau_V = \frac{1}{1-4b/3}(-\pi c\gamma_\parallel)^{-1} - \frac{4}{3}\cdot\frac{b}{1-4b/3}(-\pi c\gamma_\perp)^{-1}, \quad (30)$$

$$\tau_R = \frac{3}{4}\cdot\frac{1-4b/3}{b}\ln\left[\frac{1}{1-4b/3}\right][\pi c(\gamma_\perp - \gamma_\parallel)]^{-1}. \quad (31)$$

In this case, $G_V(t)$ and $G_R(t)$ are monotonic functions, close to exponential functions. The direct application of the Fourier transform to the experimental frequency dependences of the intensity of this line leads to the following results:[47,50]

1. At $t \leq 4$ ps, the obtained functions $G_V(t)$ and $G_R(t)$ differ only slightly from the model dependences (Lorentzian contour).

2. At $t \geq 4$ ps, the functions $G_V(t)$ and $G_R(t)$ start to be markedly dissimilar, and the rotational correlation function undergoes substantial oscillations. In our opinion, the nature of these oscillations is related to the fact that integration with respect to frequency is accomplished over finite limits (in our case, the frequency range was ~100 cm^{-1}). Then the CF in question is a convolution of the real correlation function, and the Fourier transforms from the frequency range of integration and the observed oscillations are associated with a purely mathematical effect hampering determination of physical parameters of the system such as relaxation times, angles of unit rotation of molecules, *etc.*

Similar oscillations have also been observed in the studies[9,41] of the Raman spectra and ion dynamics of OH^-, NO_3^-, and SCN^- in LiOH melts, aqueous solutions of NH_4NO_3, and also in the melts and aqueous solutions of sodium and potassium thiocyanates. It has been suggested[9,41] that the observed oscillations of $G_R(t)$ are due to the slow precession of the studied molecules. These oscillations might also be due to the pendulum motion of the molecules or to the simultaneous manifestation of the vibrational and rotational mechanisms of spectral line broadening.[51]

In view of the fact that the characteristic times of the processes considered here do not normally exceed 4 ps, it can be concluded that the Lorentzian contour describes quite adequately the actual profile of the Raman band. It is this particular contour that we used to calculate the relaxation times; in those cases where it was difficult to determine the experimental contour, it was also used to find the correlation functions.

The procedure for resolution of complex line contours in the Raman spectra

The bands for totally symmetrical stretching vibrations in the Raman spectra of XeF_2 and XeF_6 dissolved in anhydrous HF[52,53] have complex structures with several maxima, so it is difficult to obtain information on the individual components.[54] Therefore, we attempted to resolve the experimental band contours corresponding to totally symmetrical vibrations into elementary constituents. In doing this, we assumed that the approximating function has the form $y = f(x,\nu)$, where the vector x is the set of parameters to be determined: $x = \{x_n\}$ ($n = 1, 2, \ldots N$). The mathematical task was to determine x that would minimize the expression

$$\sigma^2 = \frac{1}{K}\sum_{k=1}^{K} C_k^2 [I_k - f(x,\nu)]^2 . \qquad (32)$$

Here k is the number of the frequency ν_k at which the intensity of scattered radiation I_k in the Raman spectrum was measured ($k = 1, 2, 3, \ldots$); C_k is a value characterizing the accuracy of the measurement of I; and K is the number of degrees of freedom. The $f(x,\nu)$ function has the following form[54]:

$$f(x,\nu) = \sum_{m=1}^{M} \varphi_m(x,\nu) = \frac{x_{3m-2}}{1 + (\nu - x_{3m-1})/x_{3m}} . \qquad (33)$$

The basis line, needed to take into account the background scattering, was approximated by a second-order polynomial. The reliability of the results was estimated using the Fischer test.[48,54]

It is significant that the task of resolving a complex experimental spectrum into the spectra of elementary forms in terms of known mathematical methods should be solved only in those cases where the physical reasons determining the shape of the contour are known. Otherwise, this resolution becomes a purely mathematical task, and each contour can be approximated by different numbers of components, depending on the particular algorithm used, so that it is often almost impossible to ascribe any physical meaning to these components. In addition, in this case, the accuracy of approximation would increase with an increase in the number of assumed elementary constituents.

IR spectroscopy and structural features of xenon fluorides in solutions in liquefied noble gases

The experimental procedures and equipment used in order to obtain reliable information on the molecular structure of XeF_6 took into account specific features of this compound such as its very high reactivity, which is the highest among those of xenon fluorides, its susceptibility to hydrolysis yielding an endothermic compound, XeO_3, which explodes upon slight heating, *etc.*

The nature of chemical bonds and the structure of xenon fluorides

The nature of chemical bonds in xenon fluorides has been interpreted using two models. According to one of them,[55] XeF_n are formed through excitation of the valence shell of xenon atom $Xe(5s^24d^{10}5p^6) \rightarrow Xe^*(5s^24d^{10}5p^{6-n}5d^n)$; upon excitation, xenon is capable of forming two bonds in XeF_2 ($n = 1$), four bonds in XeF_4 ($n = 2$), or six bonds in XeF_6 ($n = 3$).

In terms of the second model, formation of three-centered orbitals for four valence electrons is postulated.[56] Thus in the case of XeF_2, a p orbital of xenon partially overlaps with a p orbital of fluorine yielding bonding, nonbonding, and antibonding orbitals, which are filled by four valence electrons. Another similar orbital forms the second three-centered bond (XeF_4), and the third one forms the third three-centered bond (XeF_6). Numerous experimental data indicate[57] that the type of bonding involving substantial displacement of the spin density from the Xe atom to the F atoms is most typical of xenon fluorides.

The characteristic features of the molecular structures of xenon fluorides have been studied by vibrational

spectroscopy,[1,12,58] NMR, ESR, and photoelectron spectroscopy and by deflection of a nonfocused electron beam in a nonuniform electric field.[1,57,59,60]

The vibrational spectra of XeF_2 in the gas phase contain[1,58] three bands with frequencies of 560, 516, and 213 cm^{-1} corresponding to vibrations of a $D_{\infty h}$-structure with the types of symmetry

$$\Gamma_{vib} = \Sigma_g(\text{Raman}) + \Sigma_u(\text{IR}) + \Pi_u(\text{IR}). \quad (34)$$

The vibrational spectrum of XeF_4 in the gas phase exhibits[57,58] six bands at 585, 554, 524, 291, 218, and 161 cm^{-1}, which correspond to vibrations of a D_{4h}-structure with the types of symmetry

$$\Gamma_{vib} = A_{1g}(\text{Raman}) + A_{2u}(\text{IR}) + B_{1g}(\text{Raman}) + B_{2g}(\text{Raman}) + B_{2u}(\text{inact.}) + 2Eu_u(\text{IR}). \quad (35)$$

The geometric parameters of the molecules of xenon difluoride and tetrafluoride (R(Xe—F) = 1.979 Å, ∠F—Xe—F = 180° for XeF_2 and R(Xe—F) = 1.94 Å, R(F—F) = 2.77 Å for XeF_4), found by electron diffraction,[1,57,58] confirm the results of vibrational spectroscopy according to which XeF_2 is linear and XeF_4 is a planar square. The fact that the Xe—F bonds in XeF_2 are longer than the corresponding bonds in XeF_4 can be explained by interaction of the axial bonds with the three lone pairs occupying equatorial positions. This is in agreement with the general rule according to which an increase in the electronegativity of the central atom in a molecule results in a decrease in bond lengths.[61]

None of the structures of the other derivatives of noble gases has aroused as much discussion as the structure of XeF_6.

The molecules of XeF_6 virtually do not polymerize in the gas phase. This is indicated by the results[62] of measurements of the XeF_6 vapor density and also by the data of mass spectrometry. Only when XeF_6 was cooled by adiabatic expansion, were 10^4—10^5 cm^{-3} of the $(XeF_6)_2$ dimers, 10^3 cm^{-3} of the $R(XeF_6)$ complexes (R = He, Ne, Ar, Kr), and traces of $(XeF_6)_n$ ($n > 2$) and $R_x(XeF_6)_y$ ($x \le 2$, $y \le 2$) oligomers detected.[63]

Electron diffraction experiments[64] and analysis of the vibrational and absorption spectra in the vacuum UV region[57,58] have shown that the molecule of XeF_6 is not octahedral and its effective dipole moment is equal to zero.[60]

The main geometric configuration of XeF_6. Model concepts

There are several concepts of the structure of XeF_6. According to one of them,[65] the molecule has an octahedral structure. Another concept[66] is based on the finding that the vibrational spectra of XeF_6 exhibit more bands than it is expected for an octahedral configuration. It has been assumed that in the gas phase, XeF_6 is a mixture of three isomers, which differ in the electronic

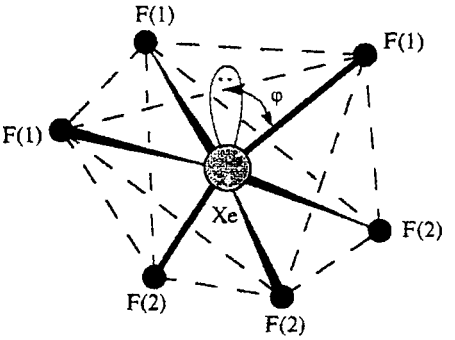

Fig. 1. Assumed geometric structure of the XeF_6 molecule in the ground (lowest) energy state (C_{3v} symmetry).

states and geometric configurations ($^1A_{1g}$, O_h; $^3A_{2u}$, D_{3d}; ^3E_u, D_{3d}) owing to the Jahn—Teller effect. However, the absorption spectra recorded[67] for XeF_6 did not confirm the presence of close (450 and 1200 cm^{-1}) electronic isomers.

According to the third concept, which has become the most popular, the XeF_6 molecule[68] is a distorted octahedron (C_{3v} symmetry) (Fig. 1). The authors of this concept proceeded from the assumption that the molecule of XeF_6 is nonrigid with respect to pseudo-rotation; as a result, four F atoms change positions, whereas the other two F atoms, which occupy *trans*-positions with respect to each other, remain in their positions.

Based on the assumption that the major configurations of XeF_6 are structures with D_{3d} or C_{3v} symmetry, three mechanisms of pseudo-rotation have been proposed:[68] the first of them transforms the D_{3d} configuration into three equivalent D_{3d} configurations and eight C_{3v} configurations; the second and the third mechanisms are similar to Berry pseudo-rotation[69] and include three and six ways of pseudo-rotation, respectively (Fig. 2). If the rotation occurs by the first mechanism, the nonrigid G_1 group is isomorphic to an O_h group. In the case of the second and third mechanisms, the nonrigid G_3 group is identical to the full permutation-inversion $G(XeF_6) = \pi_6 G_j$ group of XeF_6 molecules. Tables of characters of these groups and the selection rules in the vibration-rotational spectra of nonrigid molecules of type XY_6 have been reported previously.[68]

Xenon hexafluoride in the gas phase[66,70—74] exhibits a strong absorption band at 612 cm^{-1}, a medium band at 520 cm^{-1}, and several weak bands in the region of 400—600 and 1100—1250 cm^{-1}. The spectra of XeF_6 recorded[66] under conditions of its isolation in an Ar matrix contain several bands in the 300 cm^{-1} region. Since pseudo-rotation can lead to splitting of the levels of the main configurations, D_{3d} and C_{3v}, the qualitative spectrum of XeF_6 was calculated.[68] The frequencies were determined with calibration coefficients that provided the optimum description of the experimental vibrational spectrum of this molecule. The vibration bands in the 500—600 cm^{-1} range were assigned to transitions

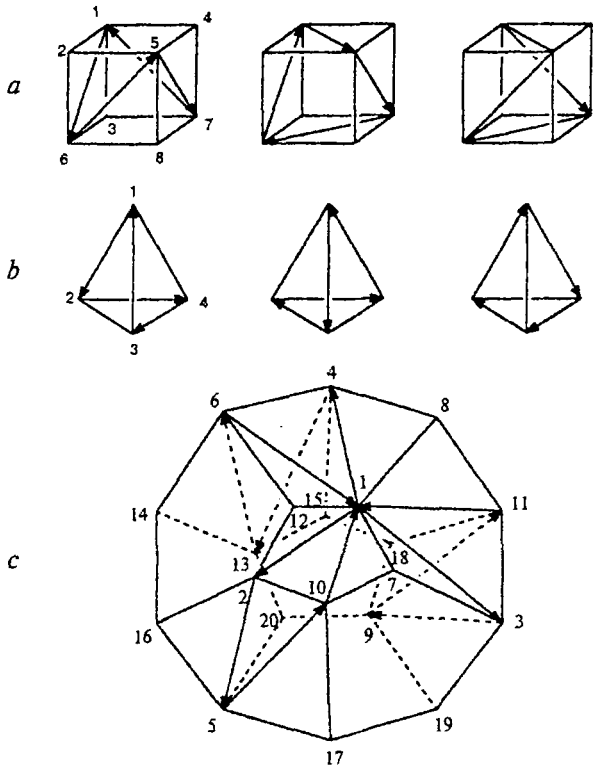

Fig. 2. Pseudo-rotations of molecules of the XY_6 type represented in terms of graphs: *a*, the first mechanism; *b*, *c*, the Berry mechanisms.

involving the states A_{1g}, E_g, and E_u (weak and medium splitting), while the bands at ~300 cm^{-1} were attributed to transitions involving the A_{1u} and E_u states (strong splitting).

The main statements concerning the structure of the XeF_6 molecule can be interpreted using the formalism of the repulsion of the valence shell electron pairs (RVSEP).[61] The structural parameters of the XeF_6 molecule are known:[75] R(Xe—F(1)) = 1.941 Å, R(Xe—F(2)) = 1.85 Å, R(F(1)—F(1)) = 3.11 Å, R(F(2)—F(2)) = 2.54 Å, and R(F(1)—F(2)) = 2.498 Å. If the molecule occurs as the C_{3v} structure, this R(F(1)—F(2)) value implies the following angles between the axis of this structure and the F atoms: 67.5° (F(1)) and 52.3° (F(2)). The corresponding angle in a regular octahedron is equal to 54.74°. In terms of the MO theory, the process of distortion of the O_h structure can be followed by looking at the MO diagram of the XeF_6 molecule[74] (Fig. 3): owing to the Jahn—Teller effect, the A^*_{1g} orbital approaches in energy the T_{1u} orbital and starts to interact with it. If the A^*_{1g}—T_{1u} interaction is strong, the symmetry of the molecule should decrease. Weak interaction between these orbitals can result only in the pronounced anharmonicity of vibrations with T_{1u} symmetry, whereas the octahedral structure can remain undistorted. In our opinion, the former situation is

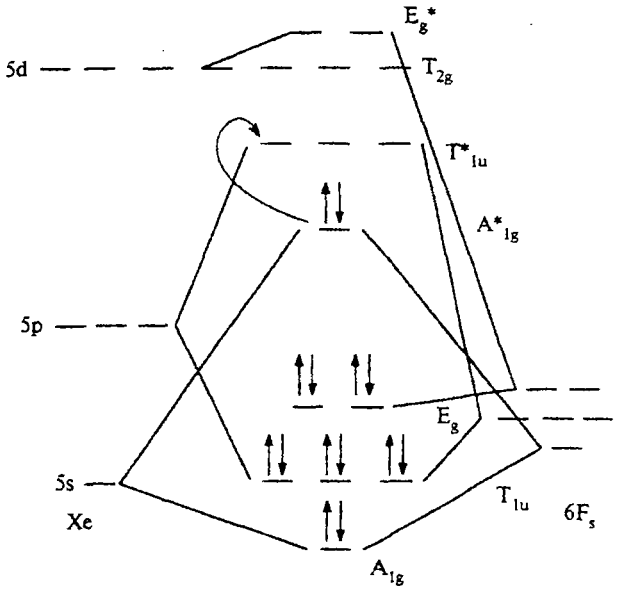

Fig. 3. Simplified diagram of the molecular orbitals in XeF_6; arrows mark the A^*_{1g}—T_{1u} interaction caused by the Jahn—Teller effect.

characteristic of XeF_6 molecules, and the latter situation characterizes $TeCl_6^{2-}$ and $TeBr_6^{2-}$ ions, which is in good agreement with the results of calculations.[76]

The nonrigidity of the XeF_6 molecule with respect to pseudo-rotation can be conveniently considered in terms of movement of the lone electron pair,[71—73] which can occur in three directions:

(a) the electron pair travels between two F atoms, and its localization exactly between them can lead to the formation of an intermediate structure with C_{2v} symmetry ($C_{3v} \rightarrow C_{2v} \rightarrow C_{3v}$ transformation accompanied by slight changes in the bond lengths and moderate changes in the angles);

(b) the electron pair migrates through the Xe—F bond in another triangular plane; if the pair points toward the F atom, XeF_6 exists as a C_{4v} structure ($C_{3v} \rightarrow C_{4v} \rightarrow C_{3v}$ transformation accompanied by a sharp increase in the length of one of the apical bonds and by small changes in the angles and in the lengths of other bonds);

(c) the electron pair passes through the center of the molecule in the direction opposite to the triangular plane; this leads to an octahedral structure ($C_{3v} \rightarrow O_h \rightarrow C_{3v}$ transformation accompanied by relatively small changes in bond lengths and angles).

Although the heights of the barriers to the above-mentioned structural rearrangements leading to the formation of intermediate structures with C_{2v}, C_{4v}, and O_h symmetries, respectively, have not been determined experimentally,[75] it has been assumed that the $C_{3v} \rightarrow O_h \rightarrow C_{3v}$ transformation is the energetically least favorable, and the potential maximum for the $C_{3v} \rightarrow C_{4v}$

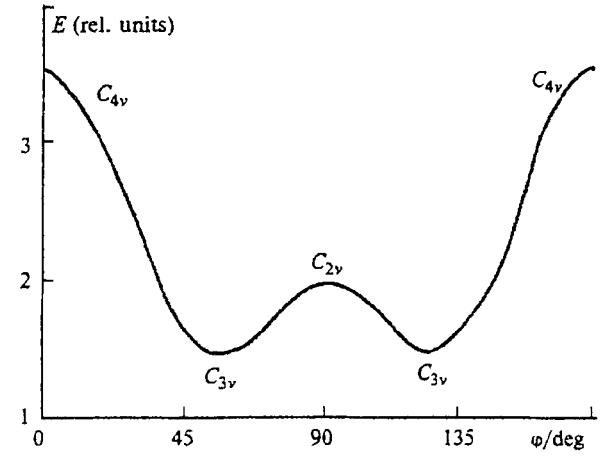

Fig. 4. Potential curve for XeF_6 depending on the angle between the Xe—F bond and the direction of the lone electron pair (φ in Fig. 1).

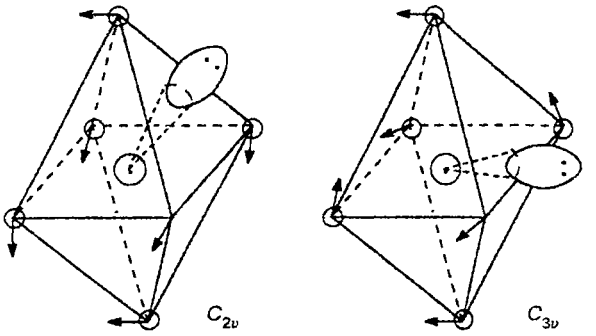

Fig. 5. Scheme of migration of the lone electron pair during the $C_{3v} \rightarrow C_{2v} \rightarrow C_{3v}$ structural transformation in XeF_6.

$\rightarrow C_{3v}$ structural transformation can be much higher than that for $C_{3v} \rightarrow C_{2v} \rightarrow C_{3v}$. This, in turn, provides grounds for assuming that the barrier to the $C_{3v} \rightarrow C_{2v} \rightarrow C_{3v}$ rearrangement can be easily overcome at the cost of thermal energy at $T = 300$ K. The geometric parameters calculated for the C_{2v} and C_{3v} configurations were reported previously,[77] and the potential curve for XeF_6 and the scheme of the lone electron pair migration during the $C_{3v} \rightarrow C_{2v} \rightarrow C_{3v}$ transformation are shown in Figs. 4 and 5.

The above-considered structurally nonrigid model of XeF_6 molecule, which assumes, in terms of the RVSEP concept, that an electron pair migrates from its position between three F atoms *via* a channel consisting of two F atoms to another position, makes it possible to interpret adequately not only most of the experimental data obtained for XeF_6 but also some characteristic features of this molecule. For example, the fact that vibrational spectra of XeF_6 exhibit no bands in the region of deformation frequencies[71—73] is apparently due to direct transformation of the deformation vibrations into pseudorotation even in the ground state. The absence of an effective dipole moment of the XeF_6 molecule is also due to its nonrigidity. The magnitude of the fixed dipole moment of XeF_6 can be[71] extremely low ($\leq 10^{-2}$ D) owing to the efficient interaction between the charges of the electron pair and the F atoms.

However, none of the models of the structure of XeF_6 considered here has been confirmed by direct experimental facts; therefore, it is impossible to choose reliably one or another geometric configuration for this molecule.

XeF_2 and XeF_4 molecules. The solubilities of XeF_2 and XeF_4 in liquid Xe are appreciably dissimilar[70—74] and are almost an order of magnitude higher[78] than their solubilities in liquid Kr.

The available experimental data[70—73,78—80] on the frequencies, half-widths, and relative intensities of the absorption bands of XeF_2 and XeF_4 in the gas phase and in solutions in liquid Kr and Xe are presented in Table 1, and the most intense vibration bands of XeF_2 and XeF_4 in the gas phase and in liquid Xe are shown in Fig. 6.

Table 1. Frequencies (ν/cm^{-1}), half-widths (Γ/cm^{-1}), and relative intensities (A_{rel}) of the absorption bands of the XeF_2 and XeF_4 molecules in the gas phase ($T = 293$ K) and in solutions in liquid Kr (LKr, $T \approx 130$ K) and Xe (LXe, $T \approx 180$ K)

Molecule	ν^{gas}	ν^{sol}		Γ^{sol}		A^*_{rel}	Assignment
		LKr	LXe	LKr	LXe		
XeF_2	—	—	504.5	—	4.2	21	ν_1 (Σ_g^+)
($D_{\infty h}$)	558.5	549.2	544.7	3.6	4.0	1000	ν_1 (Σ_u^+)
	1069.0	—	1048.2	—	4.5	63	$\nu_1 + \nu_3$
XeF_4	—	—	495.0	—	3.7	17	ν_4 (B_{2g})
(D_{4h})	585.0	575.0	571.8	3.5	3.6	1000	ν_6 (E_u)
	1105.0	—	1176.0	—	3.5	52	$\nu_4 + \nu_6$
	1136.0	—	1097.0	—	3.9	95	$\nu_1 + \nu_6$

* Intensities of the compound bands were determined in relation to the ν_3 (XeF_2) and ν_6 (XeF_4) bands, whose intensities (1000) were taken as the beginning of reference.

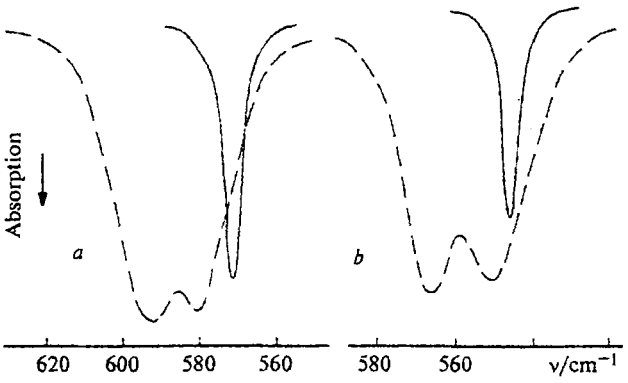

Fig. 6. Contours of the ν_6 absorption band of XeF_4 (*a*) and the ν_3 band of XeF_2 (*b*). Dashed line corresponds to the gas phase ($T = 293$ K) and the solid line corresponds to a solution in liquid xenon ($T = 180$ K).

It can be seen in Table 1 that in addition to the IR-active bands, the spectrum of XeF_4 in liquid Xe contains the ν_4 band, active in the Raman spectrum. This implies that the planar-square structure typical of XeF_4 in the gas phase is somewhat distorted on passing to a cryogenic solution. This type of distortion can occur when the dissolved molecules efficiently interact with atoms of the solvent; this is confirmed by the relatively large shift of the ν_6 frequency of XeF_4 to longer wavelengths: $(d\nu/dT) = 0.124$ cm^{-1} deg^{-1} (LXe) and 0.067 cm^{-1} deg^{-1} (LKr)[72,73,78].

The IR spectrum of XeF_2 dissolved in liquid Xe contains a band at 504.5 cm^{-1}, which was assigned to the totally symmetrical stretching mode ν_1 of the XeF_2 molecule. As in the case of XeF_4, the appearance of this Raman-active band points to a distortion of the linear structure of XeF_2; the shift of ν_3 to longer-wavelengths on passing from the gas to solution is equal to 0.115 cm^{-1} deg^{-1} (LXe) or 0.057 cm^{-1} deg^{-1} (LKr).[72,73,78]

The positions and the half-widths of the ν_3 and ν_6 bands in the IR absorption spectra of solutions of XeF_2 and XeF_4 in liquid noble gases depend on the temperature of the solution:[72,73,78–80] the temperature coefficients for the displacement of ν_3 of XeF_2 and ν_6 of XeF_4 are 0.055, 0.030 cm^{-1} deg^{-1} (LXe); 0.049, 0.027 cm^{-1} deg^{-1} (LKr), respectively (Fig. 7). The temperature-induced shifts of the maxima of the vibration bands of XeF_2 and XeF_4 were taken into account in the estimation of some anharmonicity constants X_{ik}.[70–73,79,80] Thus according to our estimates, the X_{46} value for XeF_4 is −9.0 cm^{-1}, and X_{13} for XeF_2 is −1.0 cm^{-1}. The latter value is in good agreement with the data obtained for the gas phase[57] and points to a low degree of anharmonicity of vibrations of the XeF_2 molecule.

The low-frequency shifts of the absorption bands of XeF_2 and XeF_4 following the gas—cryogenic solution transition approximately obey the additivity, which is typical of some polyatomic molecules.[15,19,28,29,81–85] This provides grounds for believing that the X_{ik} values calculated for xenon difluoride and tetrafluoride dissolved in liquid Xe are close to the corresponding values in the gas phase.

XeF_6 molecule. As in the case of XeF_2 and XeF_4, the transition from the gas phase to a solution for XeF_6 is accompanied by a shift of the fundamental band at 612 cm^{-1} to longer wavelengths; this shift amounts to 0.07 cm^{-1} deg^{-1} (LKr) and 0.18 cm^{-1} deg^{-1} (LXe)[71,73,78] (Fig. 8). In the corresponding low-temperature solutions, this band was manifested at 600 and 596 cm^{-1}. The integral absorption coefficient for the band at ~600 cm^{-1} is fairly high:[78,79] $A = (412\pm50) \cdot 10^{-8}$ cm^2 molec.$^{-1}$ s^{-1}.

An increase in the concentration of XeF_6 in cryogenic solutions leads to the appearance and growth of absorption bands at 618, 630, and 639 cm^{-1} (LXe) or 620, 634, and 645 cm^{-1} (LKr); the intensity of the fundamental band at 596 cm^{-1} (LXe) or 600 cm^{-1} (LKr) remains virtually constant (Fig. 9). Thorough measurements of the integral intensity of the fundamental band[70–73,78,79] (Fig. 10) showed that when the concentration of XeF_6 in liquid Xe is $<4.0 \cdot 10^{-4}$ mol L^{-1}, the intensity of the band at 596 cm^{-1} increases. Further increase in the concentration of XeF_6 results in a slight decrease in the intensity of this band; however, when the concentration is $>8.0 \cdot 10^{-4}$ mol L^{-1}, the intensity remains virtually constant. This behavior of the intensity of the band at 596 cm^{-1} can be explained by assuming that at low concentrations, the solution in liquid Xe mostly contains monomeric XeF_6 molecules characterized by two absorption bands at 596 and 516 cm^{-1}. It has been found[70–73] that an increase in the concentration of XeF_6 in liquid Xe results in a decrease in the quantity of monomers and appearance of a polymeric modification, which is characterized by absorption bands

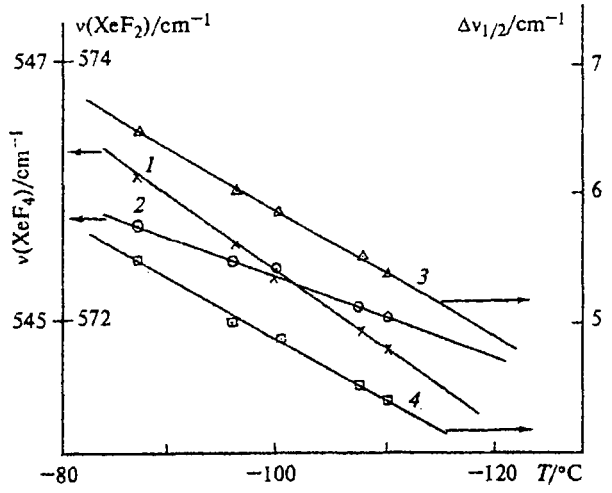

Fig. 7. Dependence of ν_3 of XeF_2 (*1*), ν_6 of XeF_4 (*2*), and their half-widths $\Delta\nu_{1/2}$ (*3* and *4*, respectively) on the temperature of the solution.

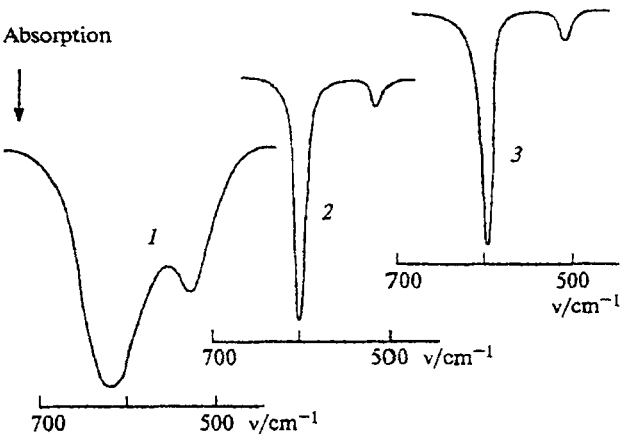

Fig. 8. Contours of the absorption bands of XeF_6 in the 500—700 cm^{-1} frequency range; gas phase (T = 293 K) (*1*), solutions in liquid krypton (T = 130 K) (*2*) and xenon (T = 180 K) (*3*).

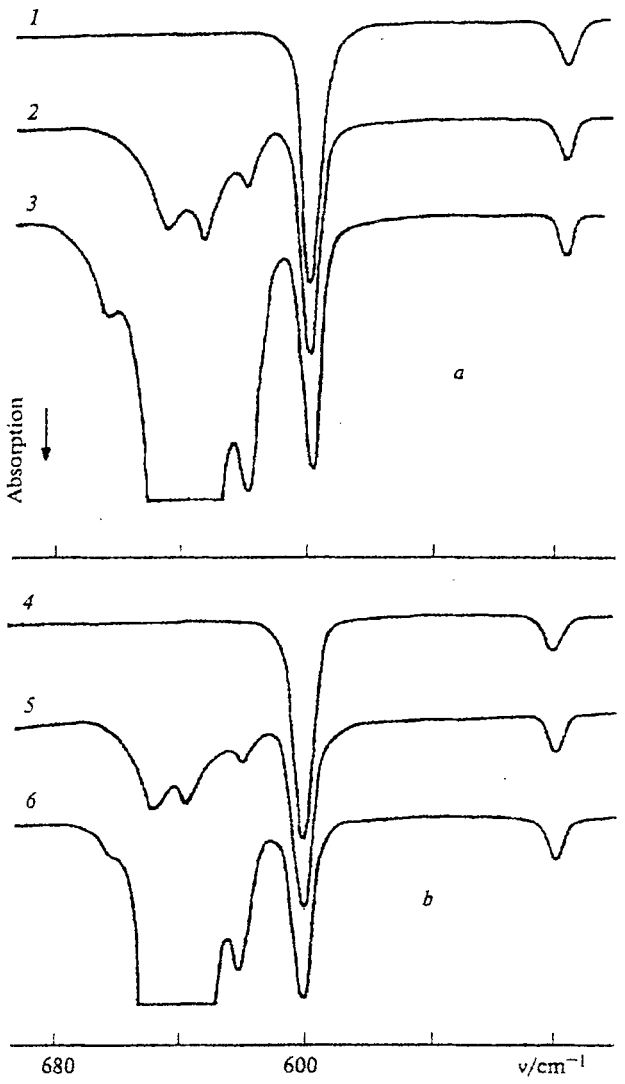

Fig. 9. IR absorption spectra of XeF_6 in solutions in liquid noble gases at 500—700 cm^{-1} at various concentrations C of xenon hexafluoride: *a*, solution in liquid Xe (T = 180 K): at $C = 1.32 \cdot 10^{-4}$ (*1*), $3.82 \cdot 10^{-3}$ (*2*), $2.57 \cdot 10^{-4}$ (*3*) mol L^{-1}, *b*, solution in liquid Kr (T = 130 K): at $C = 1.10 \cdot 10^{-4}$ (*4*), $2.91 \cdot 10^{-3}$ (*5*), $1.85 \cdot 10^{-2}$ (*6*) mol L^{-1}.

at 618, 630, and 639 cm^{-1}. These bands correspond to different orientations of the polymeric structure, and their total intensity increases nearly linearly with an increase in the concentration of XeF_6. The section on the abscissa axis intercected by the straight line *2* in Fig. 10 corresponds to the region of concentrations in which a solution in liquid Xe contains[70—73] only monomeric XeF_6.

In the case of a solution of XeF_6 in liquid Kr, polymerization starts at a lower concentration ($\sim 1.5 \cdot 10^{-4}$ mol L^{-1}), and the dependence of the intensity of the fundamental band at 600 cm^{-1} on the concentration of XeF_6 in liquid Kr resembles that observed for liquid Xe.[78,79]

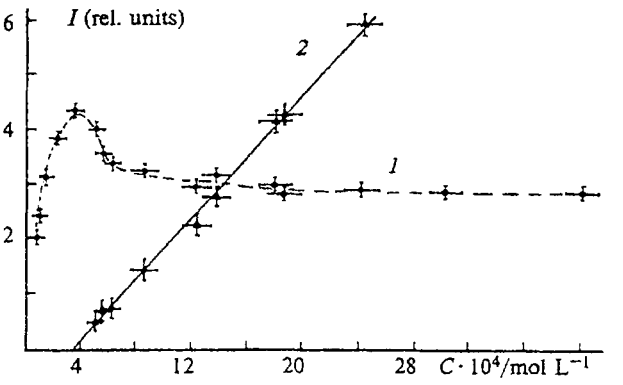

Fig. 10. Dependences of the intensities of the band at 596 cm^{-1} (*1*) and the group of bands at 620—640 cm^{-1} (*2*) on the concentration of XeF_6 in liquid Xe (T = 180 K).

The monomer—polymer equilibrium constant depends both on the temperature and on the nature of the solvent. Thus it was found[59,75] by ^{19}F and ^{129}Xe NMR spectroscopy that solutions of XeF_6 in low-polarity solvents (CF_2Cl_2, n-C_5F_{12}, F_5S—O—SF_5, CF_3Cl, *etc.*) at $T \leq 160$ K contain tetramers Xe_4F_{24}. The XeF_6 molecules might be joined into the tetramers through three-centered two-electron bonds with active participation of the lone electron pair. The Xe—Xe distance in the tetramer has been determined[76] only for the crystalline Xe_4F_{24} (4.2 Å). However, it can be expected that in solutions in low-polarity and inert solvents including liquid Kr and Xe, this distance would not markedly change. This suggests that the formation of the polymers $(XeF_6)_n$ may be due to the xenon—xenon interaction. The foregoing is supported by the finding[61,86] that the lone electron pair of the Xe atom in the $[XeF_5]^+$ cation is as stereochemically active as are those in other electron-excessive molecules like ClF_3, BrF_3, ClF_5, BrF_5, *etc.*

Along with the polymeric structures, XeF_6 dissolved in liquid Kr or Xe can form clusters $([XeF_5]^+[F]^-)_n$ (n = 2, 4). The $[XeF_5]^+$ cation should possess[61] a perfect configuration with C_{4v} symmetry. However, the lone electron pair located on the fourfold axis interacts differently with the shared electron pairs, resulting in a slight change in the angles between the shared pairs and an increase in the lengths of neighboring bonds, because the repulsion of electron *cis*-pairs is stronger than that of the *trans*-pair.[87] Consequently, the axial bond $(Xe—F)_{ax}$ in the $[XeF_5]^+$ cation becomes stronger than the equatorial bonds $(Xe—F)_{eq}$ (R_{ax} = 1.76 Å, R_{eq} = 1.84 Å, $\angle F_{ax}—Xe—F_{eq}$ = 80.4°).[88] Upon the formation of the $([XeF_5]^+[F]^-)_n$ clusters, the bridging Xe—F bonds deflect from the fourfold axis, whereas the lone electron pair can pass through a face of the XeF_5 pseudo-octahedron. This description of the formation of the $([XeF_5]^+[F]^-)_n$ clusters is in agreement with the Raman spectra of XeF_6 in WF_6 and HF solutions[87,89,90] and is

not at variance with the data on the heat capacity[91] and electrical conductivity[1] of liquid XeF_6 and its solution in HF. The above-mentioned experimental results indicate that these solutions contain the terameric phase $([XeF_5]^+[F]^-)_4$ occurring in equilibrium with the monomer $[XeF_5]^+[F]^-$ and the intermediate dimer $[Xe_2F_{11}]^+[F]^-$

$$([XeF_5]^+[F]^-)_4 + nHF \rightleftharpoons \rightleftharpoons 2[Xe_2F_{11}]^+ + (HF)_n \cdot 2[F]^-, \quad (36)$$

$$[Xe_2F_{11}]^+ + nHF \rightleftharpoons 2[XeF_5]^+ + (HF)_n[F]^-, \quad (37)$$

and that the highest proportion of the tetramer is observed in concentrated solutions of XeF_6 in HF.

In view of the fact that in reactions (36) and (37), the charges of the $[XeF_5]^+$ and $[Xe_2F_{11}]^+$ cations are counterbalanced by the charge of the $[HF_2]^-$ anions, it can be assumed that cryogenic solutions contain tetramers $(XeF_6)_4$ occurring[70–73] in equilibrium with dimers $(XeF_6)_2$ and monomers XeF_6 involving the intermediate compound $[XeF_5]^+[XeF_7]^-$:

$$(XeF_6)_4 \rightleftharpoons 2\,(XeF_6)_2, \quad (38)$$

$$(XeF_6)_2 \rightleftharpoons [XeF_5]^+[XeF_7]^-, \quad (39)$$

$$[XeF_5]^+[XeF_7]^- \rightleftharpoons 2\,XeF_6. \quad (40)$$

The most intense bands in the vibrational spectra of the $[XeF_5]^+$ cation and the $[XeF_7]^-$ anion occur[86–88,92,93] in the regions of 650 and 570–600 cm^{-1}, respectively. The IR spectra of solutions of XeF_6 in liquid Xe at high ($\geq 10^{-2}$ mol L^{-1}) concentrations exhibit[70–73] bands at 655 and 574 cm^{-1}. This indicates that at relatively low ($\leq 10^{-3}$ mol L^{-1}) concentrations of XeF_6, polymerization of the XeF_6 molecules is mostly caused by the formation of three-centered two-electron bonds between them. When the concentration of XeF_6 increases, together with the tetramerization (dimerization) process, the formation of the ionic compound $[XeF_5]^+[XeF_7]^-$ by reactions (38)–(40) can occur.

The equilibrium constants determined for the polymerization

$$n(XeF_6) \rightleftharpoons (XeF_6)_n$$

for $n = 2$ and 4 ($K = [(XeF_6)_n]/[XeF_6]^n$)[71–73] (Table 2) indicate that the equilibrium is shifted toward the formation of polymeric species $(XeF_6)_n$.

The IR absorption bands that we have assigned to the polymers $(XeF_6)_n$ occur at higher frequencies than the band corresponding to vibrations of the monomer. This shift of the band for $(XeF_6)_n$ to shorter wavelengths is apparently caused by the fact that polymerization of nonrigid molecular structures of the XF_6 type, unlike those of the classic octahedral molecules like SF_6, MoF_6, UF_6, *etc.*,[15,28,94] can result in the termination of pseudorotation. In other words, polymerization is accompanied by stabilization of complex nonrigid structures; this can occur by averaging (or retardation) of the mobility of the active F atoms. In turn, the increased structural rigidity of XeF_6 molecules can lead to an increase in the rigidity of the Xe—F bonds and thus shift the vibration bands of the polymers $(XeF_6)_n$ to lower frequencies.

Table 2. Equilibrium constants for the formation of dimers $(XeF_6)_2$ or tetramers $(XeF_6)_4$ in liquid Xe ($T = 180$ K)

$C_{XeF_6} \cdot 10^4$	$C_{(XeF_6)_n} \cdot 10^4$	$K_2 \cdot 10^{-4}$	$K_4 \cdot 10^{-11}$
mol L^{-1}		/L mol^{-1}	/L^3 mol^{-3}
1.5	2.3	1.0	4.4
1.6	2.2	0.8	3.2
1.9	8.3	2.2	5.9
2.9	17.6	2.1	2.5

At high ($\geq 10^{-3}$ mol L^{-1}) concentrations of XeF_6 in liquid Kr and Xe, the IR spectra of the cryogenic solutions exhibit bands at 1107, 1146, and 1234 cm^{-1} and at 1093, 1164, and 1230 cm^{-1}, respectively. Upon further increase in the concentration, a group of bands at 1862, 1906, and 1934 cm^{-1} (LKr) or at 1852, 1895, and 1926 cm^{-1} (LXe) appears, and the intensity of these bands is approximately half that of the bands at 1100–1200 cm^{-1}. The group of bands in the 8–9 μm range, which was observed in the gas phase when cells with large optical path lengths were used,[66] refers apparently to the $A_{1g}+E_g$, $A_{1g}+E_u$, $A_{2u}+E_u$, and E_u+E_g compound bands of monomeric XeF_6. In low-temperature solutions of XeF_6 in which the polymers $(XeF_6)_n$ predominate, this group of bands can be assigned to the first overtone of the fundamental stretching vibration of the XeF_6 incorporated in the polymer. The bands in the 1800–1900 cm^{-1} region belong most likely to the second overtone of the fundamental stretching frequencies of various orientational modifications of the polymeric structure $(XeF_6)_n$.

Thus, the results of studies of the IR absorption spectra of XeF_6 dissolved in liquid noble gases make it possible to claim that the geometry of the XeF_6 molecule in the polymeric phase differs from a regular or distorted octahedral geometry with D_{3d} symmetry. This conclusion is in agreement with the data on the energies of the ground levels of XeF_6 obtained by nonempirical calculations[95] and with the X-ray photoelectron data,[96] which indicate that the distorted octahedron with C_{3v} symmetry is the main geometry of the XeF_6 molecule.

Molecular dynamics of xenon and krypton fluorides in nonaqueous solvents

The XeF_2 molecule in MeCN, CCl_4, $(Me)_2SO$, HF, and BrF_5

In a previous study,[97] the frequency ν_1 for XeF_2 in acetonitrile (509 cm^{-1}) and the degree of depolarization

(ρ = 0.44) were determined; in addition, the XeF_2—MeCN system was found to be chemically stable. XeF_2 starts to react with MeCN at the temperature of boiling of MeCN (355.6 K).

The results of a study[1] of the vibrational spectra and ^{19}F NMR of the XeF_2—HF system and the electrical conductivity of solutions of XeF_2 in HF also indicate that these solutions are chemically stable. In the vibrational spectra of XeF_2 in nonaqueous solutions (MeCN, $MeNO_2$, CCl_4, $C_4H_8O_2$), the band for the Xe—F bond shifts[57] to lower frequencies with an increase in the electron-donating ability of the solvent.

The XeF_2—MeCN system. The Raman spectra of XeF_2 in MeCN together with the spectrum of neat MeCN are shown in Fig. 11. Analysis of the time variation of the vibrational and rotational CFs showed that the Lorentzian contour virtually coincides with the experimental contour of the ν_1 line of XeF_2. Therefore, for the XeF_2—MeCN system, we will use only the results of calculations in which $G_V(t)$ and $G_R(t)$ functions were found by simulation of the required line contour by a dispersion curve.

Table 3 presents the times of vibrational and rotational relaxation of the ν_1 mode of XeF_2 in MeCN, found from formulas (30) and (31). The same table contains the τ_j values for the M- and J-diffusion limits found using relations (24) and (25). The calculated moment of inertia (I) for free XeF_2 molecule is equal to[47,48,98] $24.71 \cdot 10^{-39}$ g cm^2. It can be seen from the data listed in Table 3 that the vibrational relaxation time is several times shorter than the rotational relaxation time at any of the studied concentrations and temperatures of MeCN solutions of XeF_2; this means that the major contribution to the broadening of the band corresponding to the totally symmetrical vibration of XeF_2 is made by vibrational dephasing.

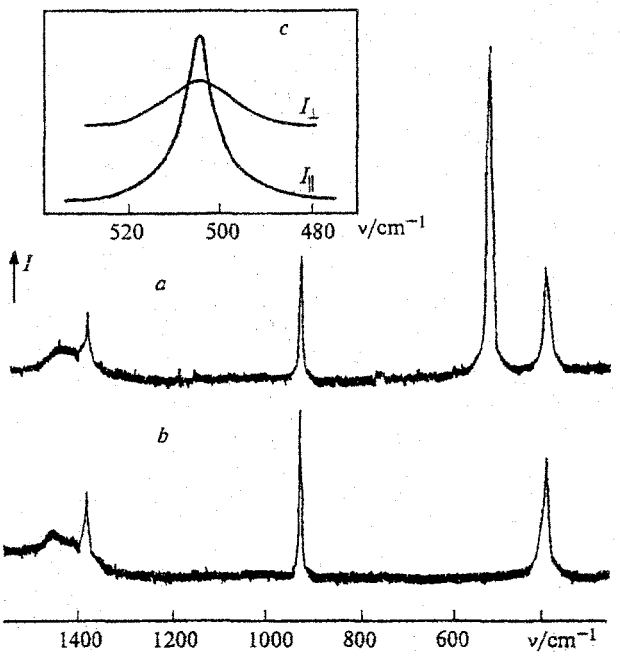

Fig. 11. Raman spectra of the XeF_2—MeCN system (C = 0.2 mol mol^{-1}, T = 300 K) (*a*) and pure MeCN (T = 300 K) (*b*) in the 250—1500 cm^{-1} range. The contours of the $\nu_1(\Sigma_g^+)$ band of the XeF_2 molecule at two mutually perpendicular polarizations (*c*).

Comparison of the vibrational correlation functions calculated from experimental data with the CFs found using formulas (21) and (22) showed that in the system under consideration, homogeneous broadening of the vibration band is realized. This makes it possible to explain the weak dependence of the τ_V value on the concentration and the temperature of the solution. In addition, realization of only one mechanism of broadening accounts for the fact that no oscillations have been detected in the initial section of the rotational correlation function, because these oscillations are generated due to simultaneous influence of both broadening mechanisms.

The forms of the CFs for various mechanisms of rotation are shown in Fig. 12, which demonstrates that the dependence of type (26) holds only starting from some instant of time, $t \approx 0.02$—0.04 ps, whereas the initial section of the plot is exponential. This behavior of the $G_R(t)$ function can be explained by the following considerations. Since small t values correspond to the sections of a line most distant from its center,[41] it is in this region that the simulation of the line contour by the Lorentzian function causes the greatest error. On moving to the center of the line, this error diminishes, and the plot of $G_R(t)$ becomes similar to the real dependence. As the time increases, the dependence of type (26) gradually approaches an exponential dependence. The time needed for this transformation to occur coincides with the time calculated for M-diffusion.

The M-diffusion approximation assumes that elastic collisions of an XeF_2 molecule with molecules of the environment predominate, although in the vast majority of cases, the mechanism of J-diffusion, which implies predominance of rotational inelastic collisions, works in

Table 3. Parameters of the vibrational and rotational relaxation of XeF_2 molecules in MeCN at various temperatures and concentrations of the solution

C /mol mol^{-1}	T/K	τ_V	τ_R	τ_j/ps		ε/deg
		ps		J-diffusion	M-diffusion	
0.1	278	1.26	2.96	0.034	0.101	7.7±1.4
	300	1.21	4.58	0.020	0.061	4.8±1.3
	323	1.40	5.03	0.021	0.064	4.2±1.3
0.05	278	1.21	2.91	0.032	0.095	5.8±1.1
	300	1.53	3.94	0.027	0.081	5.6±1.4
	323	1.30	4.04	0.025	0.074	5.8±1.3
0.02	278	1.64	1.70	0.063	0.189	13.5±1.3
	300	1.35	3.52	0.028	0.084	6.3±1.3
	323	1.04	6.70	0.014	0.041	3.2±1.3

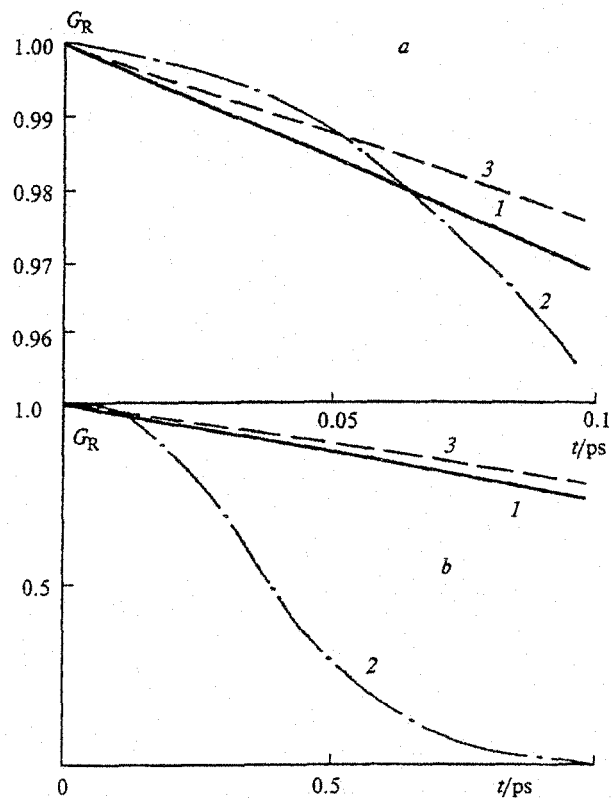

Fig. 12. Rotational CF $G_R(t)$ for the $\nu_1(\Sigma_g^+)$ mode of the XeF_2 molecule in MeCN (C = 0.05 mol mol^{-1}, T = 323 K) (*1*) and the $G_R(t)$ dependences for the mechanisms of free rotation (*2*) and rotational diffusion (*3*).

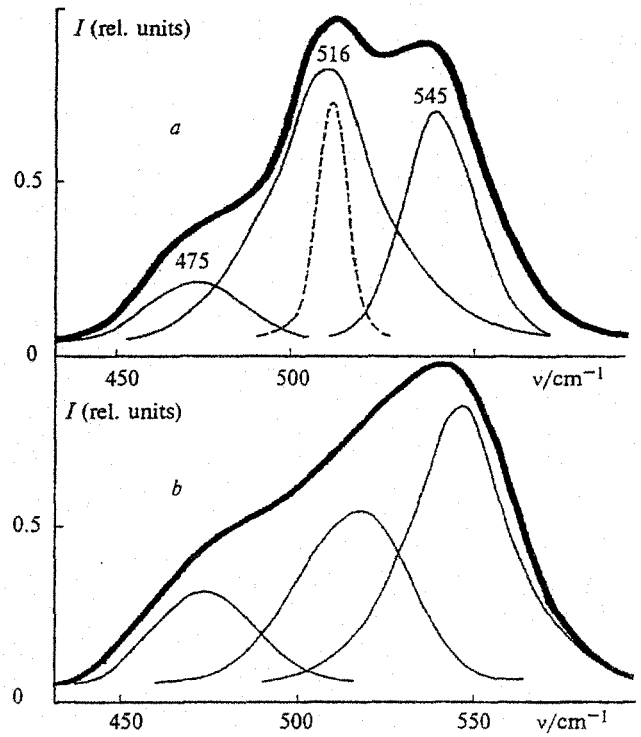

Fig. 13. Contour of the $\nu_1(\Sigma_g^+)$ line of XeF_2 in anhydrous HF (T = 300 K) at various concentrations of the solution (0.2 (*a*) and 0.09 (*b*) mol mol^{-1}) and the results of resolution of the complex Raman spectrum into elementary components. Dashed line shows the form of the $\nu_1(\Sigma_g^+)$ line of XeF_2 in the gas phase (ν_1(gas) = 515.5 cm^{-1}).

condensed systems.[40,41] This is supported by the fact that the fundamental vibration frequency of MeCN in the Raman spectrum virtually does not depend on the temperature or the concentration of the solution.

Analysis of the resulting angles of the unit rotation (ε) of an XeF_2 molecule in a MeCN solution showed that over the whole range of concentrations of XeF_2 in MeCN, the ε value decreases as the temperature of the solution increases. This can be explained by the fact that molecules of MeCN are lighter and, hence, they respond more quickly to the change in the solution temperature; therefore, when the temperature is raised, the frequency of collisions of XeF_2 with MeCN molecules increases faster than the angular velocity of their free rotation.

The XeF_2—MeCN—CCl_4 and XeF_2—MeCN—Me_2SO systems. The vibrational CFs for these systems were calculated similarly to those for the XeF_2—MeCN system. Analysis of the data indicates[47,99] that the above-listed systems are characterized by the uniform broadening of Raman lines. The calculation of rotational CFs showed that in the case of the XeF_2—MeCN—CCl_4 system, switching to the rotational diffusion regime occurs somewhat earlier ($t \approx 0.02$ ps), but also corresponds to the case of M-diffusion. As the concentration of CCl_4 increases, the vibrational and rotational relaxation times somewhat increase. This is due to the increased proportion of collisions of XeF_2 molecules with CCl_4 molecules (T_d structure), which are purely elastic and decrease the rate of relaxation processes.

In the case of the XeF_2—MeCN—Me_2SO system, the time of switching to rotational diffusion almost coincides with that found for the XeF_2—MeCN system. This result can be explained by the fact that the geometries and the main physical parameters of MeCN and Me_2SO molecules are similar.[47,99] Therefore, the change in the proportions of these solvents has only a slight influence on the rates of vibrational and rotational relaxations.

The XeF_2—HF system. Studies of the Raman spectra of XeF_2 molecules dissolved in anhydrous HF have demonstrated[49,100,101] that the ν_1 line of XeF_2 has a complicated structure with several clear-cut maxima (Fig. 13). The presence of the complex contour instead of the single ν_1 line of XeF_2, allowed for the Raman spectrum for $D_{\infty h}$ configurations by the selection rules, implies significant interaction between XeF_2 and HF. Analysis of the spectral data obtained over a broad range of concentrations of

XeF_2 in HF (0.2—0.004 mol mol^{-1})[47,49,50,100,101] showed that three elementary components with maxima at ~475, 516, and 545 cm^{-1} can be distinguished in the ν_1 mode of XeF_2. The line with the maximum at 475 cm^{-1} was attributed to the vibration of the Xe···F bridging bond in solvate systems of the XeF_2—$FXe^{\delta+}\cdots FHF^{\delta-}$ type formed due to donor—acceptor interaction of the Lewis base (XeF_2) and acid (HF). The appearance of associated XeF_2 molecules, whose contribution to the contour of this line can be fairly high, also cannot be ruled out. The line at 545 cm^{-1} is due to the $\nu_3(\Sigma_u)$ mode of bound XeF_2 having a distorted linear configuration. In addition, substantial contribution to the formation of this line contour is apparently made[47,50,100,101] by the increase in the rigidity of the Xe—F bond due to the donor—acceptor interactions, especially at low concentrations of XeF_2.

The position of the line at 516 cm^{-1} virtually coincides with the position of the ν_1 mode of XeF_2 in the gas phase; we assigned this line to the totally symmetrical Xe—F vibration in the non-bound XeF_2 molecule. The validity of this assignment is confirmed by the pattern of the dependence of the intensities and half-widths of lines on the concentration of XeF_2 in HF; as the concentration of XeF_2 decreases, the intensity of the line at 516 cm^{-1} diminishes, whereas the intensity of the line at 475 cm^{-1} increases (Fig. 14). This is due to the fact that the decrease in the concentration[49,50,100,101] leads to a decrease in the proportion of non-bound XeF_2 molecules, to destruction of the associates, and to an increase in the proportion of bound XeF_2 molecules.

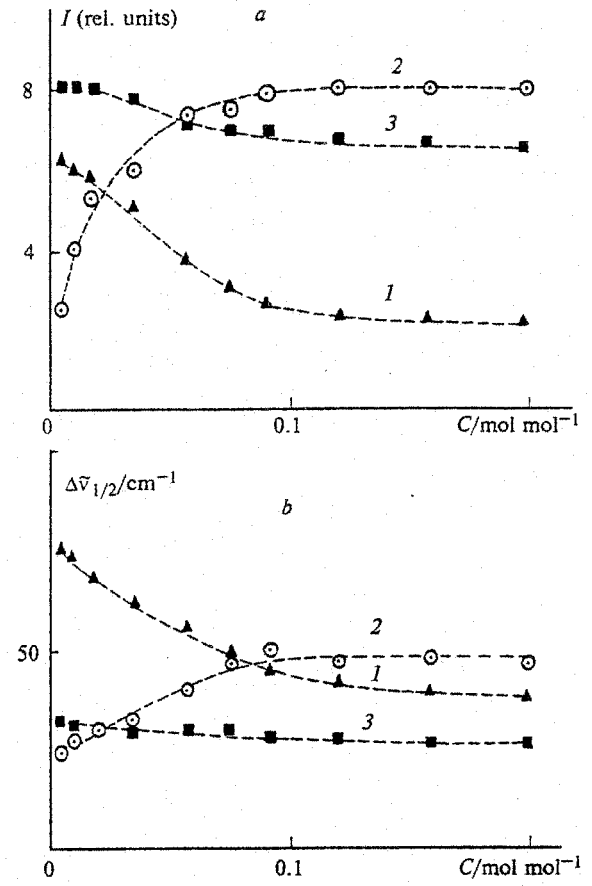

Fig. 14. Dependences of the intensities (*a*) and half-widths (*b*) of the individual components (ν = 475 (*1*), 516 (*2*), 545 (*3*) cm^{-1}) of the complex contour of the $\nu_1(\Sigma_g^+)$ line of XeF_2 in anhydrous HF (T = 300 K) on the concentration of the solution.

Table 4. Parameters of the vibrational and rotational relaxation of xenon fluorides in anhydrous HF at various concentrations of the solution (T = 300 K)

System	C /mol mol^{-1}	τ_V ps	τ_R ps
XeF_2—HF	0.20	0.28±0.05	2.28±0.20
	0.12	0.44±0.06	2.15±0.25
	0.06	0.59±0.10	1.73±0.30
	0.04	0.80±0.10	1.73±0.35
	0.009	1.12±0.20	2.64±0.45
XeF_4—HF	0.0036	0.47±0.04	0.49±0.10
	0.0021	0.48±0.10	0.50±0.15
	0.0014	0.53±0.15	0.50±0.20
XeF_6—HF	0.120	0.36±0.04	1.06±0.05
	0.063	0.37±0.07	0.89±0.08
	0.041	0.39±0.11	0.81±0.12
	0.030	0.39±0.12	0.75±0.12
	0.017	0.44±0.12	0.77±0.13
	0.008	0.50±0.15	0.61±0.15

The increase in the concentration of XeF_2 decreases the time of vibrational relaxation, whereas the time of rotational relaxation remains virtually constant (Table 4). This can be interpreted in the following way. The molecules of HF in the liquid state normally exist as zigzag-like chains $(HF)_n$ (n = 6, 7).[49,102] When these structures collide with XeF_2 molecules, the vibration energy is more likely redistributed among the identical HF molecules incorporated in the chain than between XeF_2 and individual molecules of the chain. As the concentration of XeF_2 increases, the probability of their collisions with one another increases; this leads to efficient exchange by vibrational energy resulting in acceleration of vibrational relaxation.[49,50] The rotational relaxation is mostly due to the fact that rotation of the XeF_2 molecules is hindered by collisions with associated $(HF)_n$ molecules. Since the frequency of these collisions practically does not depend on the concentration of XeF_2, the time of rotational relaxation also would not depend on the concentration of XeF_2 in HF.[47,49,50]

The form of the rotational CF $G_R(t)$ for different mechanisms of rotation of XeF_2 in HF solutions is similar to the pattern of $G_R(t)$ for the XeF_2—MeCN system. The time at which the regime of free rotation is replaced by rotational diffusion corresponds to the time calculated for the case of J-diffusion. An estimate of the angle of rotation of XeF_2 at the first step of diffusion has

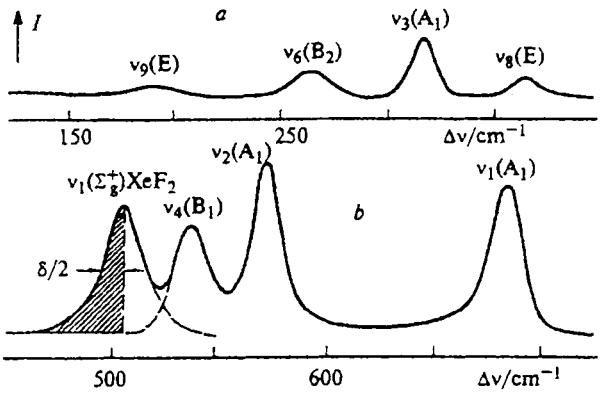

Fig. 15. Raman spectrum of the XeF_2—BrF_5 system (C = 0.17 mol mol^{-1}, T = 300 K) in the 150—400 cm^{-1} range (*a*) and 450—750 cm^{-1} range (*b*). The hatched section of the contour of the $\nu_1(\Sigma_g^+)$ line of XeF_2 was used to find the CF.

shown that the ε value practically does not change over the whole studied range of concentrations of XeF_2 in HF and lies in the 9—12° range.

The XeF_2—BrF_5 system. The Raman spectra of solutions of XeF_2 in BrF_5, unlike those of the XeF_2—HF system, over a fairly broad range of concentrations of XeF_2 (0.22—0.046 mol mol^{-1}), exhibit a single line with a maximum at 508 cm^{-1} corresponding to the ν_1 mode of XeF_2 (Fig. 15).

To find the CF, only the contours of bands obtained at high (0.22—0.15 mol mol^{-1}) concentrations of the solution were considered. At lower concentrations, the line contour of interest corresponding to XeF_2 overlaps with the contour of the BrF_5 line with $\nu_4(B_1)$ = 535 cm^{-1},

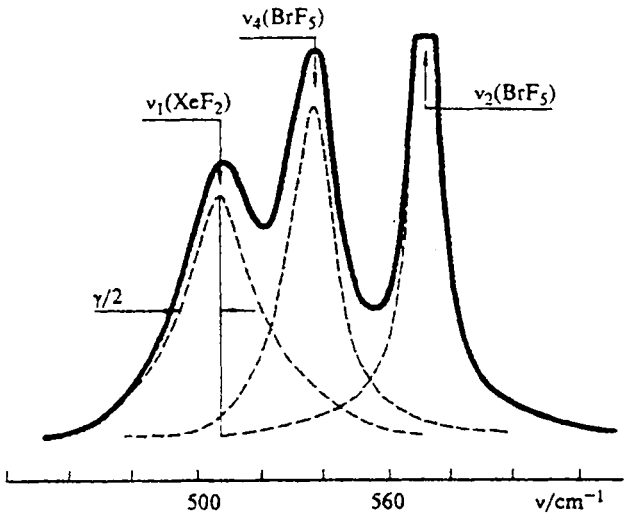

Fig. 16. Contour of the $\nu_1(\Sigma_g^+)$ line of XeF_2 in BrF_5 (C = 0.13 mol mol^{-1}, T = 300 K). Dashed line shows the individual components obtained by the resolution of the complex experimental contour.

which is much more intense in the Raman spectra (Fig. 16).

The times of vibrational and rotational relaxation were found to be of the same order of magnitude and equal to 0.40 and 1.84 ps, respectively, *i.e.*, the major contribution to the formation of the contour of the ν_1 mode of XeF_2 is made by the vibrational dephasing.

Comparison of the CFs obtained for the fast and slow modulations indicate that at $t \leq 0.4$ ps, the mechanism of inhomogeneous broadening predominates, whereas at $t \geq 0.6$ ps, the uniform broadening mechanism mostly works. The replacement of inhomogeneous broadening by uniform broadening is due to the fact that at small t values ($t \leq 0.2$ ps), the average squared frequency fluctuation is much larger than τ_v^{-1}. Therefore, the environment of the XeF_2 molecules can be considered to be a quasi-static system. As t increases, the fluctuation contribution decreases, and the Raman band is broadened as a result of movement of the surrounding species.

As in the case of the XeF_2—HF system, in the XeF_2—BrF_5 system, J-diffusion occurs, and the rotation angle of the XeF_2 molecule at the first step of diffusion (ε) amounts to ~3.0°.

XeF_4 in HF solutions. Only one publication was devoted to the Raman spectra of XeF_4 molecules in a solution in anhydrous HF;[1] in this study, the Raman line at 550 cm^{-1} corresponding to vibrations of the Xe—F bond was observed. In the same study, based on the measurements of the electrical conductivity of solutions of XeF_4 in HF and also on the ^{19}F NMR spectra, it was concluded that XeF_4 forms a molecular solution in HF and that the XeF_4—HF system is chemically stable.

The Raman spectra of solutions of XeF_4 in HF, unlike those of the XeF_2—MeCN and XeF_2—HF systems, have been obtained in a fairly narrow concentration range (0.0036—0.0014 mol mol^{-1}) due to the poor solubility of XeF_4.

The correlation functions $G_V(t)$ and $G_R(t)$ for the $\nu_1(A_{1g})$ mode of XeF_4 molecules in HF, calculated using the two procedures described above, are fairly close to one another. In this system, unlike the above-described systems, the times of vibrational and rotational relaxation found assuming the Lorentzian profile of the $\nu_1(A_{1g})$ line of XeF_4 are almost identical over the whole studied range of concentrations of XeF_4 in HF (see Table 4). This indicates that both vibrational and rotational relaxation equally participate in the formation of the ν_1 line contour of XeF_4. Analysis of the limiting $G_V(t)$ dependences for the homogeneous and inhomogeneous types of broadening indicates that both mechanisms of broadening influence the formation of the XeF_4 ν_1 contour, but the fast modulation noticeably predominates. Since in the case where only the uniform broadening mechanism acts, the band is described by the Lorentzian contour, it is obvious that in our case, the profile of the ν_1 line of XeF_4 is close to the dispersion contour. This accounts for the fact that the CFs for the model and experimental contours differ only slightly.

Analysis of the rotational CF calculated based on the experimental contours and also for free rotation and rotational diffusion shows that the initial section of the $G_R(t)$ plot ($t \leq 0.35$ ps) is a parabola corresponding to free rotation with an effective moment of inertia nearly equal to that of a free XeF_4 molecule ($I = 47.49 \cdot 10^{-39}$ g cm^2).[51] This finding can be explained by the fact that the solutions in question, unlike the XeF_2—HF system, contain no associates of the XeF_4—$(HF)_n$ type.

For the XeF_4—HF system, the time needed to switch to the regime of rotational diffusion corresponds to the limiting case of J-diffusion, and the angle of rotation (ε) at the first step of diffusion in the concentration range considered almost does not change and amounts to ~10°.

XeF_6 in HF solutions. Xenon hexafluoride acts not only as a Lewis base, for example

$$XeF_6 \rightarrow [XeF_5]^+ + F^-, \quad (41)$$

$$XeF_6 + [XeF_5]^+ \rightarrow [Xe_2F_{11}]^+ \quad (42)$$

but also as a Lewis acid[58]

$$XeF_6 + nF^- \rightarrow [XeF_{6+n}]^{n-}. \quad (43)$$

The typical properties of an amphoteric compound are manifested when XeF_6 is associated in the liquid phase:

$$2\,XeF_6 \rightleftharpoons [XeF_5]^+ + [XeF_7]^- \rightleftharpoons (XeF_6)_2, \quad (44)$$

the Trooton constant for this process is[58] 33.9 kcal mol^{-1} deg^{-1}. The formation of the above and also more complex associates[89] is apparently favorable from the energy viewpoint;[57,58] this may be due to the fact that $[XeF_5]^+$, $[XeF_7]^-$, and other similar ions possess a higher symmetry than XeF_6. In particular, the energy gain upon the formation of the $[XeF_5]^+$ cation (a tetragonal pyramid with C_{4v} symmetry)[92,93] from XeF_6 (a distorted octahedron with C_{3v} symmetry)[72,73] is manifested in the fact that XeF_6 possesses the highest electron-donating ability among Xe fluorides, although a comparison of the energies of formation of the cations

$$XeF_n \rightarrow [XeF_{n-1}]^+ + F^- \ (n = 2, 4, 6) \quad (45)$$

and their radii ($R_{[XeF]^+} < R_{[XeF_3]^+} < R_{[XeF_5]^+}$), which determine the crystal lattice energy, implies[57,89] that XeF_2 should be the strongest base (the most efficient donor of the F^- ions).

The chemical shifts in the ^{19}F NMR spectra of solutions of XeF_6 in HF[59] and WF[58] depend on the temperature, which has been explained[58] by the fact that the solutions contain both monomeric and polymeric forms of XeF_6 in which all the Xe and F atoms are magnetically equivalent.[59,75]

The abnormally high electrical conductivity of solutions of XeF_6 in HF indicates that it is substantially ionized in solution[86]

$$XeF_6 + HF \rightarrow XeF_5^+ + HF_2^-. \quad (46)$$

The Raman spectra of XeF_6 in the gas phase are characterized[66] by a very intense band at 513 cm^{-1}, intense polarized bands at 102, 582, and 613 cm^{-1}, and an intense depolarized band at 69 cm^{-1}. The Raman spectra of liquid XeF_6 exhibit bands at 650 (s), 577 (m), 506 (w) cm^{-1}, and in the case of solid XeF_6, bands at 656 (s), 636 (m), and 583 (w) cm^{-1} are observed.

In the Raman spectra of solutions of XeF_6 in anhydrous HF, bands with maxima at 660, 620, and 600 cm^{-1} were detected.[1,87] Previously,[87] the Raman spectra of complexes of XeF_6 with acceptors of F^- ions (BF_3, PdF_4, PF_5, AsF_5, PtF_5, *etc.*) were studied both in the solid state and in HF solutions; the frequencies of the $[XeF_5]^+$ and $[Xe_2F_{11}]^+$ cations and the $[BF_4]^-$, $[PF_6]^-$, $[AsF_6]^-$, $[PdF_6]^{2-}$, *etc.* anions were assigned.

The Raman spectra of the XeF_6—HF system appreciably depend on the concentration of XeF_6. Based on the data on the structure of solid XeF_6,[76] it was suggested[87] that a molecule of XeF_6 should be regarded as an ionic compound of the $[XeF_5]^+[F]^-$ type. Based on the analysis of the vibrational spectra of the compounds $[XeF_5]^+[XF_6]^-$ and $[Xe_2F_{11}]^+[YF_6]^-$ (X = As, Pd, Ru, Pt; Y = As, P), it was also concluded that in concentrated solutions (XeF_6 : HF ≈ 1 : 10, mol mol^{-1}), the tetramer $([XeF_5]^+[F]^-)_4$ predominates; at moderate concentrations (XeF_6 : HF ≈ 1 : 20, mol mol^{-1}), the dimer $([XeF_5]^+[F]^-)_2$ is the major species; finally, at low concentrations (XeF_6 : HF ≈ 1 : 150, mol mol^{-1}), the solution contains mostly the monomer $[XeF_5]^+[F]^-$. Thus, the processes occurring in the XeF_6—HF system can be described by reactions (36) and (37). This assumption is in line with the data[1] on the electrical conductivity of solutions of XeF_6 in HF and also with the results of NMR studies[59,75] of the XeF_6—HF system.

Vibrational spectrum of the $[XeF_5]^+$ cation. In order to understand the mechanisms of the processes occurring in the XeF_6—HF system, it is necessary to take into account the amphoteric properties of XeF_6 and also to obtain detailed information on the vibrational spectrum of the $[XeF_5]^+$ cation in an HF solution. However, data of this sort concerning $[XeF_5]^+$, unlike those for its isoelectronic analogs, IF_5, $[TeF_5]^-$, and $[SbF_5]^{2-}$,[12,103] are scarce. The interpretation of vibrations of $[XeF_5]^+$ based on the data[87,104] of the vibrational spectra of $[XeF_5]^+[BF_4]^-$ and $[XeF_5]^+[AsF_6]^-$ is contradictory as regards assignment of Xe—F vibration frequencies in the 200—400 cm^{-1} range both for solids and for their solutions in anhydrous HF. In addition, the assignment of frequencies in the vibrational spectra of $[XeF_5]^+$ recorded in previous studies[105,106] also cannot be regarded as reliable, because it was based on the results[87] obtained almost without polarization measurements in the Raman spectra.

Therefore, we studied the vibrational spectra of the $[XeF_5]^+$ cation in the solid state (as $[XeF_5]^+[AsF_6]^-$,

$[XeF_5]^+[PbF_4]^-$, and $[XeF_5]^+[MnF_5]^-$) and in solution in HF (as $[XeF_5]^+[AsF_6]^-$) and also considered systematically the published data.[92,93]

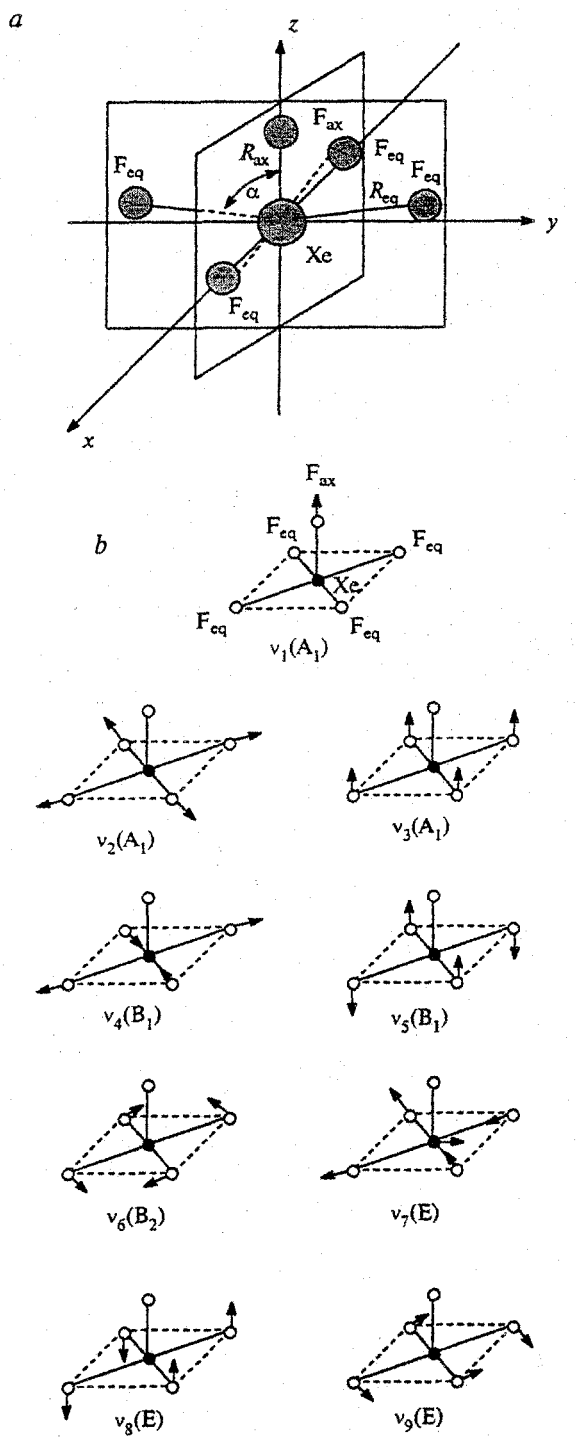

Fig. 17. Geometric structure (*a*) and normal modes (*b*) of the $[XeF_5]^+$ cation: R_{ax} = 1.76 Å, R_{eq} = 1.84 Å, α = 80.4°.

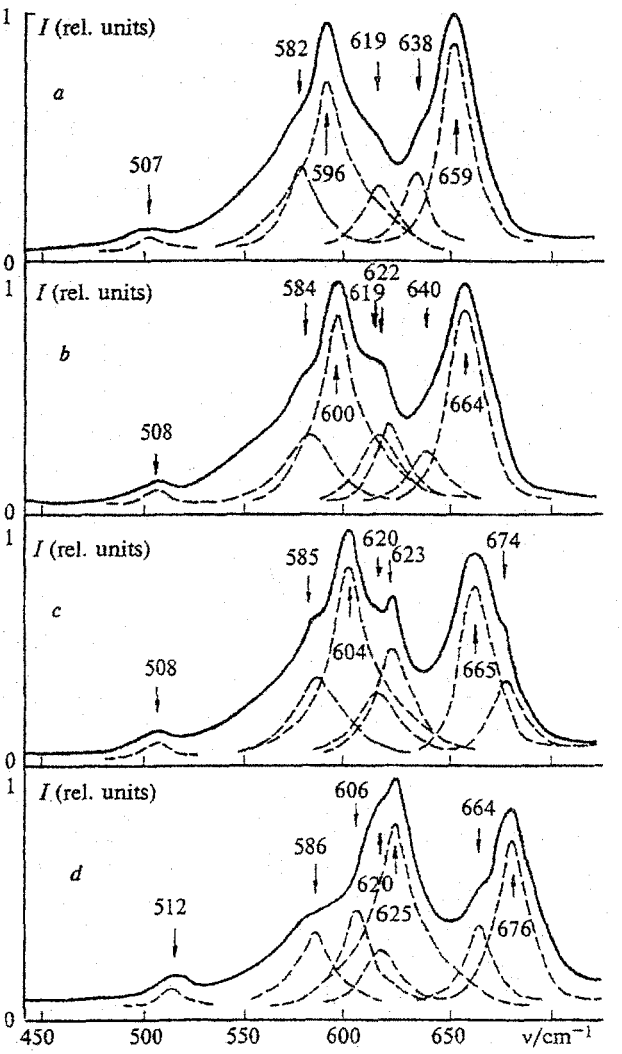

Fig. 18. Raman spectra of the xenon hexafluoride in anhydrous HF at T = 293 K in the 450—750 cm^{-1} range (concentration of the solution 0.12 (*a*), 0.063 (*b*), 0.024 (*c*), 0.0083 (*d*) mol mol^{-1}). Dashed line shows the individual components obtained by the resolution of the complex experimental contour.

The vibrational spectrum of $[XeF_5]^+$, like that of $[XeCl_5]^+$,[8,107] contains nine bands corresponding to the C_{4v} configuration (tetragonal pyramid); all nine lines of the cation are active in the Raman spectrum, and only six vibrations with A_1 and E symmetry are IR-active. In the Raman spectrum of $[XeF_5]^+$, only those bands are polarized that correspond to vibrations with A_1 symmetry.

The available data on the vibrational spectra of the $[XeF_5]^+$ cation in the solid phase have been compared[92,93] with the data for solutions in anhydrous HF; based on calculations of the normal modes of molecules of the XY_5 type (C_{4v}), detailed interpretation of these data was accomplished.[107—109] Figure 17 presents sche-

Table 5. Vibrational frequencies (ν/cm^{-1}) and their assignments in the Raman spectra of the XeF_6—HF system at various concentrations of XeF_6 in the solution ($T = 293$ K)

0.12*	0.063*	0.024*	0.0083*	Assignment
—	—	674 sh, p	676 s, p	$[XeF_5]^+F^-$
—	664 s, p	664 s, p	664 sh, p	$([XeF_5]^+F^-)_2$
659 s, p	—	—	—	$([XeF_5]^+F^-)_4$
638 sh, p	640 w, p	—	—	$[XeF_5]^+[XeF_7]^-$
—	622 sh, p	623 sh, p	625 s, p	$[XeF_5]^+F^-$
619 sh, p	619 sh, p	620 sh, p	620 sh, p	XeF_6
—	600 s, p	604 s, p	605 sh, p	$([XeF_5]^+F^-)_2$
596 s, p	—	—	—	$([XeF_5]^+F^-)_4$
582 sh, p?	584 sh, p?	585 sh, p?	586 sh, p?	$(F_5Xe)^{\delta-}\cdots(FHF)^{\delta-}$
507 w, dp	508 w, dp	508 w, dp	512 w, dp	XeF_6
408 w, dp	410 w, dp	410 w, dp	411 w, dp	$[XeF_5]^+F^-$,
359 w, p	360 w, p	361 w, p	361 w, p	$([XeF_5]^+F^-)_2$ or
206 w, dp	208 w, dp	205 w, dp	200 w, dp	$([XeF_5]^+F^-)_4$

Note. p are polarized Raman lines, dp are depolarized lines.
* Concentration of XeF_6 in HF/mol mol^{-1}.

matically the geometric structure and the normal modes for the $[XeF_5]^+$ cation shaped like a tetragonal pyramid.

As noted above, according to the views developed previously[87] and also to the currently available data[76] on the structure of solid XeF_6 and models of its structure in the liquid phase,[59,75,86] a monomeric XeF_6 molecule in a highly polar solvent such as HF can be regarded as the ionic compound $[XeF_5]^+[F]^-$, whereas polymeric forms of XeF_6 are represented by dimers $([XeF_5]^+[F]^-)_2$ and tetramers $([XeF_5]^+[F]^-)_4$. The Raman spectra exhibit a polarized line at 618 cm^{-1} and a depolarized line at 507 cm^{-1} over the whole range of XeF_6 concentrations in HF (0.12—0.075 mol mol^{-1}), and a decrease in the concentration of XeF_6 is accompanied by slight shifts of these lines to shorter wavelengths, *viz.*, to 620 and 512 cm^{-1}, respectively (Fig. 18, Table 5). In accordance with the results of IR-cryospectroscopic studies,[70—73,78—80] we assigned these lines to vibrations of the Xe—F bonds in nonionized XeF_6 molecules. The bands at 596 and 659 cm^{-1} (see Fig. 18, *a*), 600 and 664 cm^{-1}, and 604 and 665 cm^{-1} (see Fig. 18, *b,c*) were assigned to the stretching vibrations of the nonionized tetramer $([XeF_5]^+[F]^-)_4$ and dimer $([XeF_5]^+[F]^-)_2$, respectively; the higher-frequency bands can be attributed to vibrations of the $(Xe—F)_{ax}$ bonds, and the lower-frequency bands were ascribed to vibrations of the $(Xe—F)_{eq}$ bond in the $[XeF_5]^+$ cation incorporated in the polymer $([XeF_5]^+[F]^-)_n$ ($n = 2, 4$). Strictly speaking, this assignment cannot be regarded as sufficiently reliable, although it is in good agreement with the assignment reported[87] for the $[Xe_2F_{11}]^+$ cation. In cannot be ruled out that in addition to the tetramer $([XeF_5]^+[F]^-)_4$ and the dimer $([XeF_5]^+[F]^-)_2$, a solution of XeF_6 in HF contains ionic compounds such as $[XeF_5]^+[XeF_7]^-$; these compounds have been detected[70—73] in studies of the IR spectra of solutions of XeF_6 in liquid Kr and Xe. This statement is supported by the fact that the Raman spectra of concentrated solutions of XeF_6 in HF exhibit a polarized line in the region of 640 cm^{-1} (see Fig. 18, *a,b*); according to the previously reported data[86] on the vibrational spectra of NO_2XeF_7, we assigned this line to the symmetrical stretching vibration of $[XeF_7]^-$. Note that we did not detect the low-intensity lines at 520 and 560 cm^{-1}, which had been observed previously[86] and assigned to the deformation vibrations of $[XeF_7]^-$. A band at 580 cm^{-1} was observed in the Raman spectra; this band was attributed to the vibration of the bridging Xe···F bond in solvate systems[92,93] $(XeF_6)_m—([F_5Xe]_n^{\delta+}\cdots n[FHF]^{\delta-})$ (A) (*m* and *n* can vary from 1 to 4, so that $m + n \leq 4$), which are formed as a result of donor—acceptor interactions between a Lewis base and a Lewis acid; however, this band might also be due to the $\nu_4(B_1)$ stretching mode of the $[XeF_5]^+$ cation incorporated into an ionized polymeric group.

The maxima of the Raman bands corresponding to the vibrations of the $[XeF_5]^+$ cation in the spectra of solutions of $[XeF_5]^+[BF_4]^-$, $[XeF_5]^+[AsF_6]^-$, and $[XeF_5]^+[F]^-$ in HF virtually coincide[89,93] (Table 6). This means that not only the lengths of strong axial bonds $(Xe—F)_{ax}$ and the weaker equatorial bonds (Xe—

Table 6. Vibrational frequencies and their interpretation in the Raman spectrum of the $[XeF_5]^+F^-$ monomer in anhydrous HF ($T = 293$ K)

0.024*	0.0083*	Assignment ($[XeF_5]^+$)
674 sh, p	676 c, p	ν_1 (A_1), stretching Xe—F_{ax}
623 sh, p	625 c, p	ν_2 (A_1), in-phase stretching, XeF_4
361 w, p	361 w, p	ν_3 (A_1), in-phase out-of-plane deformation, XeF_4
410 w, dp	411 w, dp	ν_8 (E), deformation, F_{ax}—Xe—F_{eq}
205 w, dp	200 w, dp	ν_9 (E), deformation, XeF_4

Note. p are polarized Raman lines, dp are depolarized lines.
* Concentration of XeF_6/mol mol^{-1}.

$F)_{eq}$, but also the $F_{ax}—Xe—F_{eq}$ angles in the above compounds are identical. For isoelectronic analogs of the $[XeF_5]^+$ cation, the angles between the axial and equatorial bonds are also close to one another[92,93] (IF_5, 81.7°; TeF_5^-, 78.8°; SbF_5^{2-}, 79.4°) pointing to hybridization of the central atomic orbitals.

Using spectroscopic data obtained previously and the known structural parameters,[88] we estimated the force constants of $[XeF_5]^+$ by the reported procedure.[110—112] The following values were obtained: f_R = 4.32± 0.2 mdyne Å^{-1}, f_r = 3.97±0.2 mdyne Å^{-1}, f_α = 0.75± 0.15 mdyne Å^{-1}, and f_β = 2.25±0.2 mdyne Å^{-1}; the $f_{\alpha\alpha}$, $f_{\beta\beta}$, and $f_{r r}$ values do not exceed 0.1 mdyne Å^{-1}. The resulting f_R, f_r, f_α, and f_β values are in good agreement with the results of previous calculations,[104] whereas the interaction constants are somewhat different. Thus the $f_{r r}$ value varied in the 0.29—0.54 mdyne Å^{-1} range, depending on the calculation procedure; $f_{\beta\beta}$ was found to be 0.15 mdyne Å^{-1}, and in the case of $f_{\alpha\alpha}$ = −0.05 mdyne Å^{-1}, even the sign changed.[104] This suggests that consideration of the force field of $[XeF_5]^+$ requires allowance for the intramolecular interactions, for example, those between F_{ax} and F_{eq}.

Dynamic characteristics of the XeF_6 molecule in HF. The vibrational and rotational CF of the Raman lines with maxima at 596—625 cm^{-1} corresponding[89,90] to the vibrations of nonbound ionized molecules, $([XeF_5]^+F^-)_n$ (n = 1, 2, 4), calculated by two procedures, are fairly close to each other. This allowed determination of the characteristic times of vibrational and rotational relaxation (see Table 4). The vibrational relaxation time for the Xe—F vibrations in ionized $([XeF_5]^+F^-)_n$ molecules (n = 1, 2, 4) depend only slightly on the concentration of XeF_6 in HF; it increases ~1.5-fold as the concentration of XeF_6 decreases by more than an order of magnitude. This is due to the nonrigidity of the XeF_6 molecule with respect to pseudorotation. Therefore, the τ_V value can serve as a sort of characteristic of the mobility of the F atoms in the monomeric and polymeric $([XeF_5]^+F^-)_n$ forms. Theoretical estimates[113,114] have shown that the characteristic times of intramolecular rearrangements in $([XeF_5]^+F^-)_n$ (n = 1, 2, 4) do not exceed 0.35±0.15 ps. In addition, some increase in the vibrational relaxation time upon an increase in the concentration of XeF_6 can be associated with the transformation of the monomers $([XeF_5]^+F^-)$ into polymeric forms $([XeF_5]^+F^-)_n$ (n = 2, 4); this, in turn, can markedly increase the cross-section of the process of formation of ion pairs such as $[XeF_5]_n^+[FHF]^-$. This assumption is in good agreement with the views developed[40,41,115] in relation to concentrated aqueous solutions of nitrates and thiocyanates, which contain a wide diversity of species (contact ion pairs and more complex assemblies) resulting from strong inter-particle interactions.

The characteristic time of rotational relaxation τ_R at high concentrations of XeF_6 in HF is ~3 times longer than τ_V. A decrease in the concentration of XeF_6 results in a decrease in the τ_R value, and at a concentration of ~0.008 mol mol^{-1}, τ_R becomes nearly equal to τ_V. This can be explained by the retardation of the rotation of the particles in question upon the transformation of the monomeric phase ($[XeF_5]^+F^-$) into polymers as a result of collisions with associated solvent molecules $(HF)_n$ (n = 6, 7) and also by the enhancement of the interaction of the $[XeF_5]^+$, $[Xe_2F_{11}]^+$, *etc.* cations both with one another and with the F^-, $(HF)_n$, and $[XeF_7]^-$ species and type A associates.

Analysis of the vibrational CFs $G_V(t)$ and also the CFs obtained in terms of fast and slow modulation for three modifications of $([XeF_5]^+F^-)_n$[89] indicates that in the case of the tetramer, the slow modulation mechanism predominates at $t \le 0.2$ ps, while the fast modulation mechanism mostly works at $t \ge 0.3$ ps. In the case of dimers, the former and the latter mechanisms act at $t \le$ 0.45 ps and $t \ge 0.5$ ps, respectively. Finally, for the monomer, the mechanism of slow modulation is active at $t \le 0.65$ ps, whereas the mechanism of uniform broadening is switched on at $t \ge 1.0$ ps. The increase in the time interval needed for the change in the character of band broadening on going to monomer is due to the fact that the monomers experience a lesser influence of the neighbors (solvent molecules and the assemblies present in the solution) than the dimers or tetramers.[89]

Comparison of $G_R(t)$ with $G_{FR}(t)$ and $G_{RD}(t)$ for the monomer $[XeF_5]^+F^-$ showed that it rotates as a free rotator at $t \le 0.2$ ps, and switches to the rotation diffusion regime at $t \ge 0.4$ ps. These values correspond to the case of J-diffusion. The angle of rotation (ε) of $[XeF_5]^+F^-$ at the first step of diffusion amounts to ~10±3°.

KrF_2 in solutions of HF and BrF_5. The molecule of KrF_2, like XeF_2, is linear (R(Kr—F) = 1.889±0.01 Å, R(F—F) = 3.781 Å), which is indicated by the results of electron diffraction studies of KrF_2 in the gas phase and by the data of vibrational spectroscopy.[57,116] The vibrational spectrum of KrF_2 contains three bands with frequencies ν_1 = 449 cm^{-1}, ν_2 = 233 cm^{-1}, and ν_3 = 588 cm^{-1} (gas) and ν_1 = 462 cm^{-1}, ν_3 = 580 cm^{-1} (solid), which correspond to vibrations of a $D_{\infty h}$ structure.[116] It has been noted[57,116,117] that the force constant is negative, $f_{r r}$ = −0.2 mdyne Å^{-1}, and that there is no Fermi resonance between the ν_1 and $2\nu_2$ states. The IR spectra of solid and matrix-isolated KrF_2 at low temperatures contain[1] absorption bands at 520, 536, and 573 cm^{-1}; the former two bands were assigned[116] to polymeric modifications of KrF_2, while the latter was attributed to the monomeric molecule. Studies of the ^{19}F NMR spectrum of krypton difluoride dissolved in anhydrous HF have shown[58,116] that the F atoms in KrF_2 are magnetically equivalent; no exchange between the F atoms of KrF_2 and HF has been noted even at 300 K. Based on the studies of ^{19}F NMR spectra and chemical properties of KrF_2, it was concluded[57] that the KrF_2—HF and KrF_2—BrF_5 systems are chemically stable. The chemical bond in KrF_2 is usually described[1] in

terms of delocalized molecular orbitals built as a combination of the p_σ orbitals of Kr and F. As a rule, one filled $4p_\sigma$ orbital of Kr and two atomic $2p_\sigma$ orbitals of F are considered, although it cannot be ruled out[57] that, unlike Xe—F, the Kr—F bonds contain some contribution of the 2s orbitals of F and 4d orbitals of Kr. The results of ^{19}F NMR studies of KrF_2—HF solutions imply[58,116] that the variation in shielding coefficients can be related to the degree of covalency of bonds and to the electronegativities of atoms making up the molecules in question. Calculations with allowance for p_σ bonds[58] showed that the charge distributions between the F and noble gas atoms can be represented as $Xe^{+1.58}(F^{-0.79})_2$ and $Kr^{+0.94}(F^{-0.47})_2$. Hence, the bonds in KrF_2 are more covalent than those in XeF_2. The linear KrF_2 and XeF_2 molecules can be treated as resonance hybrids of three contributing structures, two of which are ionic and one of which is covalent:[117]

$$\underset{\mathbf{I}}{F{-}X^+F^-} \leftrightarrow \underset{\mathbf{II}}{F^-X^+{-}F} \leftrightarrow \underset{\mathbf{III}}{\overline{FXF}}. \qquad (47)$$

Since the energy of the X—F bond in XeF_2 is ~2.5 times greater than that[58] in KrF_2, the contribution of structure **III** to the total energy is larger in the case of KrF_2. In addition, the difference between the electronegativies of Xe and F atoms is larger than that between Kr and F atoms. This results in the larger ionicity of the bond in XeF_2 and may be among the reasons that account for the formation of chemical bonds between XeF_2 and HF molecules in solutions in anhydrous HF.

The KrF_2—HF system. Studies of the Raman spectra of KrF_2 dissolved in HF have shown[50,118,119] that the spectra of the KrF_2—HF system, unlike those of the XeF_2—HF system, contain one band, which is in agreement with the selection rules for linear molecules with $D_{\infty h}$ symmetry. The vibrational and rotational CFs for the ν_1 mode of KrF_2 in an HF solution are close to each other. Based on the assumption that the contour of the ν_1 line of KrF_2 in HF is described by a dispersion curve, the vibrational and rotational relaxation times for this vibration were determined (Table 7).[50,118,119] The time of rotational relaxation τ_R is several times longer than the vibrational relaxation time τ_V over the whole range of concentrations of KrF_2 in anhydrous HF; in other words, as in the case of solutions of XeF_2 in MeCN, HF, and BrF_5, the greatest contribution to the formation of the contour of the ν_1 line of KrF_2 is made by the vibrational dephasing. In addition, when the concentration of KrF_2 in HF increases, the τ_V value slightly decreases, whereas τ_R remains virtually constant. This result can be explained in the same way as in the case of the XeF_2—HF system.

The calculation of the limiting $G_V(t)$ dependences for the homogeneous and inhomogeneous broadening showed[118,119] that at $t \le 0.6$ ps, the slow modulation mechanism predominates, whereas at $t \ge 1.2$ ps, uniform broadening is observed in the KrF_2—HF system. The change in the mechanism of broadening is due to the same reasons as those in the XeF_2—BrF_5 and XeF_4—HF systems. Comparison of $G_R(t)$ with $G_{FR}(t)$ and $G_{RD}(t)$ demonstrates that at $t \le 0.09$ ps, a KrF_2 molecule in anhydrous HF rotates as a free rotator, but as early as at $t \ge 0.25$ ps, the rotational diffusion regime is switched on. The angle of rotation of a KrF_2 molecule in HF at the first step of diffusion differs only slightly from the corresponding value for XeF_2—HF and amounts to ~8—10°, and the time at which the system passes to rotational diffusion corresponds to the case of J-diffusion.

Table 7. Parameters of the vibrational and rotational relaxation of KrF_2 in anhydrous HF and BrF_5 at various concentrations of the solution (T = 293 K)

System	C /mol mol^{-1}	τ_V ps	τ_R ps
KrF_2—HF	0.30	0.47±0.05	2.10±0.10
	0.11	0.53±0.07	2.39±0.15
	0.053	0.64±0.10	2.12±0.25
	0.012	0.58±0.15	1.93±0.30
	0.004	0.71±0.20	2.43±0.30
KrF_2—BrF_5	0.97	0.82±0.05	2.14±0.05
	0.42	0.97±0.05	2.02±0.10
	0.17	0.91±0.10	1.98±0.15
	0.04	0.94±0.20	1.62±0.20

Based on semiclassical theoretical views, we calculated the potentials of intermolecular interaction of KrF_2 and XeF_2 molecules with HF molecules within the framework of a relatively simple electrostatic model.[120,121] The shift of the vibration frequencies of XF_2 (X = Kr, Xe) following their interaction with HF molecules was found from the following expression

$$\Delta\nu(R, \theta_R, \varphi_R, \theta_{r_2}, \varphi_{r_2}) = \\ = \pm\nu_0(\partial^2 U_0/\partial r^2)|_{r_1}/2(\partial^2 U/\partial r^2)|_{r_1}, \qquad (48)$$

where R is the distance between HF and XF_2 molecules, r_1 and r_2 are lengths of the X—F and H—F bonds, respectively, U is the potential energy of the XF_2—HF intermolecular interaction, U_0 is the potential energy of interatomic interaction in an isolated linear XF_2 molecule, and θ and φ are azimuthal and polar angles with respect to the axis Z, respectively. Averaging of the shift $\Delta\nu$ over all possible orientations of the XF_2 and HF molecules gave the statistical average $\nu(R)$ value; in this case, the spectra of the KrF_2 and XeF_2 molecules were represented as sets of δ-functions for each chosen set of frequencies:

$$\delta(\Delta\nu - \nu_0 U''_0/2U'') = \\ = \lim t/\pi[(\Delta\nu - \nu_0 U''_0/2U'')^2 + t^2]. \qquad (49)$$

The results of the calculations demonstrated that the calculated contour for the KrF_2—HF system is close to the experimental profile, whereas in the case of the XeF_2—HF system, the model and the real contours are

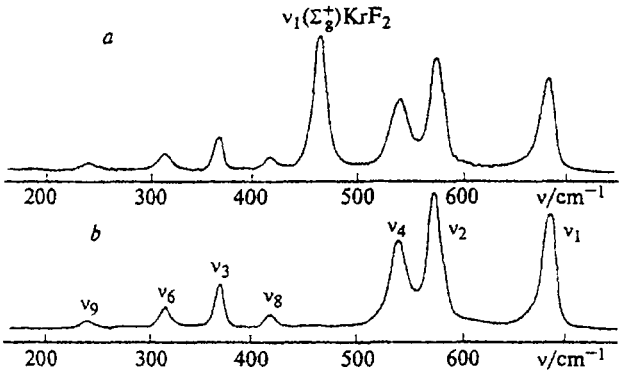

Fig. 19. Raman spectra at T = 293 K of the KrF_2—BrF_5 system (C = 0.27 mol mol^{-1}, T = 293 K) (*a*) and pure BrF_5 (*b*) in the 150—750 cm^{-1} range.

different. This is additional evidence for the occurrence of solvation effects, which have a substantial influence on the energy and spectral parameters of the XeF_2—HF system. In addition to the linear solvation processes, whose description is based on the assumption of the linear character of polarization of the solvent in the field of a solute molecule, a considerable contribution of nonlinear solvation processes is also possible. The latter type of processes manifested in solutions in high-polarity solvents result in the appearance of local areas with ordered molecular structure, which is due to the interaction between permanent and induced dipoles.[121]

The KrF_2—BrF_5 system. The Raman spectra of the KrF_2—BrF_5 system at room temperature were recorded in the 0.97—0.04 mol mol^{-1} range of concentrations (Fig. 19).[118] The vibrational and rotational CFs calculated using Fourier transforms of the experimental and Lorentzian contours are close to one another. Estimation of the vibrational and rotational relaxation times shows that over the whole range of concentrations of KrF_2, the time τ_R is more than twice τ_V (see Table 7). This indicates that, as in the KrF_2—HF system, in this case, too, the vibrational dephasing process makes the greatest contribution to the formation of the contour of the ν_1 band of KrF_2 in BrF_5. The slight increase in the τ_R value following an increase in the concentration of KrF_2 can be explained[118,119] by the fact that the rotation is restricted by enhancement of the interaction of KrF_2 molecules with BrF_5 and also by the formation of the adducts $KrF_2 \cdot BrF_5$.

Comparison of the $G_V(t)$ functions with the CFs found within the limits of fast and slow modulations shows that at $t \leq 0.45$ ps, the mechanism of inhomogeneous broadening predominates in the formation of the contour of the ν_1 line of KrF_2 in BrF_5, and at $t \geq 1.9$ ps, the broadening becomes homogeneous. The time intervals characterizing the regimes of free rotation and rotational diffusion in the KrF_2—BrF_5 system (0.03 and 0.5 ps) are virtually identical to those found for the XeF_2—BrF_5 system (0.04 and 0.5 ps). Taking into account the fact that the moment of inertia (I) of KrF_2 amounts to[118,119] $22.53 \cdot 10^{-39}$ g cm^2, the angle of unit rotation of this molecule at the first step of diffusion was found to be ~3.5°. Since the time it takes for the system to get out of the free rotation regime and the time characterizing the frequency of collisions with the surrounding particles are close to each other, it can be concluded that in the KrF_2—BrF_5 system, as in the KrF_2—HF system, J-diffusion occurs.

* * *

Study of the vibrational spectra of noble gas fluorides in cryogenic and nonaqueous solutions shows that in liquid xenon the molecular structures of XeF_2 ($D_{\infty h}$) and XeF_4 (D_{4h}) are distorted, and allows us to calculate the anharmonicity constants for some vibrations of these molecules.

An increase in the concentration of XeF_6 in cryogenic solutions ($\geq 4 \cdot 10^{-4}$ and $1.5 \cdot 10^{-4}$ mol L^{-1} for liquid xenon and krypton, respectively) results in the formation of polymeric structures $(XeF_6)_n$ (n = 2, 4) and an ionic compound, $[XeF_5]^+[XeF_7]^-$. The equilibrium constants for polymerization were calculated, and it was shown that the main configuration of the XeF_6 molecule is that of a distorted octahedron (with C_{3v} symmetry).

Taking into account the results of polarization measurements of the bands for totally symmetrical stretching vibrations in the Raman spectra of KrF_2, XeF_2, XeF_4, and XeF_6 dissolved in MeCN, Me_2SO, CCl_4, HF, and BrF_5, the vibrational and rotational CFs were calculated by Fourier transforms of the experimental and model band contours. Assuming that the line contour is described by a Lorentzian, analytical expressions for the CFs and for the vibrational and rotational relaxation times were obtained.

The mechanisms of the formation of lines in the Raman spectra of noble gas fluorides in nonaqueous solvents were established. The time intervals during which the systems pass from slow modulation to fast modulation and the time intervals in which the molecules rotate as free rotators were determined. The angles of unit rotations of molecules at the first step of diffusion were estimated.

In the XeF_2—HF and XeF_6—HF systems, a number of associates such as XeF_2—$FXe^{\delta+} \cdots FHF^{\delta-}$ and $(XeF_6)_m$—$([F_5Xe]_n^{\delta+} \cdots n[FHF]^{\delta-})$ and ionic compounds resulting from donor—acceptor interaction of Lewis bases with Lewis acids were found.

The results obtained make it possible to take into account the structural features of noble gas fluorides in predicting their behavior in chemical reactions with various organic and inorganic compounds and to determine the character of interaction of dissolved compounds with solvent molecules, and also to obtain data on the effect of these interactions on the kinetic parameters of the main chemical process.

This work was carried out with the financial support of the Russian Foundation for Basic Research (Project No. 96-03-34250).

References

1. *Noble Gas Compounds*, Ed. H. H. Hyman, the University of Chicago Press, Chicago—London, 1963.
2. B. B. Chaivanov, Sh. Sh. Nabiev, V. B. Sokolov, and S. N. Spirin, *J. Fluor. Chem.*, 1991, **54**, 12.
3. N. C. Yang, T. C. Shien, E. D. Feit, and C. L. Chernic, *J. Org. Chem.*, 1970, **35**, 4020.
4. V. V. Chaivanov, V. B. Sokolov, and S. N. Spirin, *Sb. nauchn. trudov IAE* [*Collection of Scientific Works of the Institute of Nuclear Energy*], 1989, 86 (in Russian).
5. B. M. Smirnov, *Uspekhi Fiz. Nauk* [*Advances in Physics*], 1983, **139**, 53 (in Russian).
6. S. L. Vershinin and M. F. Churbanov, *Vysokochist. veshchestva* [*High-Purity Substances*], 1993, No. 5, 15 (in Russian).
7. J. E. Huheei, *Inorganic Chemistry. Principles of Structure and Reactivity*, Harper and Row Publ., New York, 1983.
8. Sh. Sh. Nabiev and L. P. Sukhanov, *Zh. Fiz. Khim.* [*Russ. J. Phys. Chem.*], 1997, **71**, 1969.
9. M. H. Brooker and G. H. Papatheodorou, *Adv. Molten Salt Chem.*, Elsevier, New York, 1983, **5**, 26.
10. Sh. Sh. Nabiev, *Preprint IAE* No. 5100/12, Kurchatov Institute of Nuclear Energy, Moscow, 1990, 119 pp. (in Russian).
11. Sh. Sh. Nabiev, *Preprint IAE* No. 5310/12, Kurchatov Institute of Nuclear Energy, Moscow, 1991, 87 pp. (in Russian).
12. N. Smyrl and G. Momantov, *Adv. Inorg. Chem. Radiochem.*, 1978, **21**, 231.
13. M. O. Bulanin, *J. Mol. Struct.*, 1973, **19**, 59.
14. Sh. Sh. Nabiev, B. G. Sartakov, V. P. Ushakov, V. V. Klimov, N. B. Afanas'ev, A. P. Osipov, and A. E. Varfolomeev, *Zh. Prikl. Spektr.*, 1990, **52**, 234 [*J. Appl. Spectr.*, 1990, **52** (Engl. Transl.)].
15. *Molekulyarnaya Kriospektroskopiya* [*Molecular Cryospectroscopy*], Ed. M. O. Bulanin, Izd. Sankt-Peterburgskogo Univ., St. Petersburg, 1993, 300 pp. (in Russian).
16. L. A. Zhigula, T. D. Kolomiitsova, V. A. Kondaurov, S. M. Melikova, and D. N. Shchepkin, *Zh. Prikl. Spektr.*, 1992, **56**, 381 [*J. Appl. Spectr.*, 1992, **56** (Engl. Transl.)].
17. Sh. Sh. Nabiev, V. D. Klimov, and B. S. Khodjiev, *J. Fluor. Chem.*, 1992, **58**, 291.
18. V. A. Kondaurov, S. M. Mel'nikova, Sh. Sh. Nabiev, D. A. Raldugin, P. G. Sennikov, and D. N. Shchepkin, *Vysokochist. veshchestva* [*High-Purity Substances*], 1993, No. 3, 119 (in Russian).
19. Sh. Sh. Nabiev and B. S. Khodzhiev, *Zh. Neorg. Khim.*, 1994, **39**, 1702 [*Russ. J. Inorg. Chem.*, 1994, **39** (Engl. Transl.)].
20. J. Turner and M. Poliakoff, *Fres. J. Anal. Chem.*, 1986, **324**, 819.
21. Sh. Sh. Nabiev and V. P. Ushakov, *IV Vsesoyuzn. konf. po khimii nizkikh temperatur* [*IV All-Union Conf. on the Low-Temperature Chemistry*], Abstrs., Izd. MGU, Moscow, 1988, p. 217 (in Russian).
22. Sh. Sh. Nabiev and B. S. Khodzhiev, *Preprint IAE* No. 5723/12, Kurchatov Institute of Nuclear Energy, Moscow, 1993, 20 pp. (in Russian).
23. Sh. Sh. Nabiev, D. A. Raldugin, V. A. Revin, P. G. Sennikov, and B. S. Khodzhiev, *Vysokochist. veshchestva* [*High-Purity Substances*], 1994, 77 (in Russian).
24. Sh. Sh. Nabiev, P. G. Sennikov, D. A. Raldugin, V. A. Revin, and B. S. Khodjiev, *Spectrochim. Acta*, 1996, **52A**, 453.
25. Ya. M. Kimel'fel'd, *Usp. Khim.*, 1988, **57**, 1273 [*Russ. Chem. Rev.*, 1988, **57** (Engl. Transl.)].
26. Sh. Sh. Nabiev, B. G. Sartakov, and V. P. Ushakov, *Preprint IAE* No. 4892/12, Kurchatov Institute of Nuclear Energy, Moscow, 1989, 28 pp. (in Russian).
27. Sh. Sh. Nabiev, *Preprint IAE* No. 4973/12, Kurchatov Institute of Nuclear Energy, Moscow, 1989, 20 pp. (in Russian).
28. Sh. Sh. Nabiev and V. D. Klimov, *Mol. Phys.*, 1994, **81**, 395.
29. Sh. Sh. Nabiev, B. G. Sartakov, V. P. Ushakov, V. V. Klimov, G. L. Odabashyan, A. P. Osipov, and S. V. Sin'ko, *Zh. Prikl. Spektr.*, 1990, **52**, 405 [*J. Appl. Spectr.*, 1990, **52** (Engl. Transl.)].
30. V. D. Klimov, T. D. Kolomijtsova, V. A. Kondaurov, S. M. Melikova, Sh. Sh. Nabiev, and D. N. Schepkin, *Abstr. XXI Europ. Congress on Molec. Spectrosc.*, Tech. Univ. Publ., Vienna, 1992, E34.
31. Sh. Sh. Nabiev, *Proc. XIII Intern. Conf. on High Resol. Molec. Spectrosc.*, Osrodek Wydawnictw Naukowych, Poznan, 1994, J2.
32. P. G. Sennikov, D. A. Raldugin, and Sh. Sh. Nabiev, *Abstr. XII Symp. on High Resol. Molec. Spectrosc.* (Petergof, 1996), Sankt-Petersburg Univ. Publ., Petergof, 1996, 32.
33. P. G. Sennikov, D. A. Raldugin, and Sh. Sh. Nabiev, *Izv. Akad. Nauk, Ser. Khim.*, 1996, 2259 [*Russ. Chem. Bull.*, 1996, **45**, 2144].
34. S. Cradock and A. Hinchcliffe, *Matrix Izolation*, Cambridge University Press, Cambridge, 1975.
35. V. V. Klimov, A. V. Mamchenko, Sh. Sh. Nabiev, and L. P. Sukhanov, *Zh. Fiz. Khim.*, 1991, **65**, 1819 [*Russ. J. Phys. Chem.*, 1991, **65** (Engl. Transl.)].
36. V. D. Klimov, A. V. Mamchenko, Sh. Sh. Nabiev, and L. P. Sukhanov, *Proc. 13th Intern. Conf. on Raman Spectrosc.*, Wiley, New York, 1992, 718.
37. A. Smith, *Applied Infrared Spectroscopy*, Wiley and Sons, New York, 1979.
38. Sh. Sh. Nabiev and V. P. Ushakov, *Sb. nauchn. trudov IAE* [*Collection of Scientific Works of the Institute of Nuclear Energy*], Moscow, 1989, 92 (in Russian).
39. C. H. Wang, *Spectroscopy of Condensed Media*, Academic Press, New York, 1985, 321 pp.
40. W. P. Rothschild, *Dynamics of Molecular Liquids*, Wiley, New York, 1984, 417 pp.
41. S. A. Kirillov, *Dinamicheskie svoistva molekul i kondensirovannykh sistem* [*Dynamic Properties of Molecules and Condensed Systems*], Ed. A. N. Lazarev, Nauka, Leningrad, 1988, 190 (in Russian).
42. Sh. Sh. Nabiev, I. I. Ostroukhova, N. A. Revina, and L. P. Sukhanov, *Izv. Akad. Nauk, Ser. Khim.*, 1997, 961 [*Russ. Chem. Bull.*, 1997, **46**, 921].
43. R. G. Gordon, *J. Chem. Phys.*, 1966, **44**, 1830.
44. A. Carrington and A. D. McLachlan, *Introduction to Magnetic Resonance*, Harper & Row Publ., New York, 1967.
45. R. E. D. McClung, *J. Chem. Phys.*, 1971, **55**, 3459.
46. P. S. Habbard, *Phys. Rev.*, 1974, **A6**, 2421.
47. Sh. Sh. Nabiev and I. I. Ostroukhova, *Vysokochist. veshchestva* [*High-Purity Substances*], 1993, 111 (in Russian).

48. Sh. Sh. Nabiev and I. I. Ostroukhova, *Spectrochim. Acta*, 1993, **49A**, 1527.
49. Sh. Sh. Nabiev and I. I. Ostroukhova, *Spectrochim. Acta*, 1993, **49A**, 1537.
50. Sh. Sh. Nabiev and I. I. Ostroukhova, *Proc. Symp. "Strukturno-dinamicheskie protsessy v neuporyadochennykh sredakh" [Structural and Dynamic Processes in Disordered Media]*, Izd. Samarkandskogo Univ., Samarkand, 1992, part 1, 39 (in Russian).
51. Sh. Sh. Nabiev and I. I. Ostroukhova, *Preprint IAE* No. 5607/12, Kurchatov Institute of Nuclear Energy, Moscow, 1993, 16 pp. (in Russian).
52. Sh. Sh. Nabiev and I. I. Ostroukhova, *Preprint IAE* No. 5406/12, Kurchatov Institute of Nuclear Energy, Moscow, 1991, 15 pp. (in Russian).
53. Sh. Sh. Nabiev, *Preprint IAE* No. 5615/12, Kurchatov Institute of Nuclear Energy, Moscow, 1993, 28 pp. (in Russian).
54. G. S. Denisov and B. S. Terushkin, *Molekulyarnaya spektroskopiya [Molecular Spectroscopy]*, Izd. LGU, Leningrad, 1981, issue 5, 232 (in Russian).
55. R. Catton and K. Mittchell, *Can. J. Chem.*, 1970, **48**, 2695.
56. R. Harcourt and A. Harcourt, *J. Chem. Soc., Faraday Trans. 2*, 1974, **70**, 743.
57. A. B. Neiding and V. B. Sokolov, *Usp. Khim.*, 1974, **43**, 2145 [*Rus. Chem. Rev.*, 1974, **43** (Engl. Transl.)].
58. H. Bartlett and F. O. Sladky, *Comprehensive Inorg. Chem.*, Eds. J. C. Bailar and A. F. Trotman, Pergamon Press, New York, 1973, **1**, 213.
59. K. Seppelt, *Acc. Chem. Res.*, 1979, **12**, 211.
60. W. E. Falconer, M. J. Vasile, and F. A. Stevie, *J. Chem. Phys.*, 1977, **66**, 5335.
61. R. J. Gillespie, *Molecular Geometry*, Van Nostrand Reinold Comp., London, 1972.
62. B. Weinstock, E. Weaver, and C. Knop, *Inorg. Chem.*, 1966, **5**, 2189.
63. M. J. Vasile and F. A. Stevie, *J. Chem. Phys.*, 1981, **75**, 2399.
64. R. M. Gavin and L. S. Bartell, *J. Chem. Phys.*, 1968, **48**, 2460.
65. T. H. Brown, P. H. Kasai, P. H. Werner, and E. B. Whipple, *J. Chem. Phys.*, 1964, **40**, 3448.
66. H. H. Claassen, G. Goodman, and H. Kim, *J. Chem. Phys.*, 1972, **56**, 5042.
67. E. W. Philips, J. W. D.Coholly, and S. B. Trickey, *Chem. Phys. Lett.*, 1972, **17**, 203.
68. C. Trindle, S. N. Datta, and T. D. Bouman, *Intern. J. Quant. Chem.*, 1977, **11**, 627.
69. A. I. Boldyrev and O. P. Charkin, *Zh. Strukt. Khim.*, 1984, **25**, 102 [*J. Struct. Chem.*, 1984, **25** (Engl. Transl.)].
70. Sh. Sh. Nabiev, *Sb. nauchn. trudov IAE [Collection of Scientific Works of the Institute of Nuclear Energy]*, Kurchatov Institute of Nuclear Energy, Moscow, 1990, **1**, 117 (in Russian).
71. Sh. Sh. Nabiev, V. D. Klimov, and B. S. Khodzhiev, *Preprint IAE* No. 5170/12, Kurchatov Institute of Nuclear Energy, Moscow, 1990, 27 pp. (in Russian).
72. Sh. Sh. Nabiev, V. D. Klimov, and B. S. Khodjiev, *J. Fluor. Chem.*, 1991, **54**, 344.
73. Sh. Sh. Nabiev, V. V. Klimov, and B. S. Khodzhiev, *Zh. Fiz. Khim.*, 1991, **65**, 2125.
74. Sh. Sh. Nabiev and V. D. Klimov, *Proc. X Symp. and School on High Resol. Molec. Spectrosc.* (Omsk, 1990), SPIE Publ., Washington, 1991, **1811**, 248.
75. K. Seppelt and D. Lentz, *Progr. Inorg. Chem.*, 1982, **29**, 167.
76. R. D. Burbank and G. R. Jones, *J. Am. Chem. Soc.*, 1974, **96**, 43.
77. M. Klobukowski, S. Husinaga, L. Sejio, and Z. Barandiaran, *Theor. Chim. Acta*, 1987, **62**, 237.
78. Sh. Sh. Nabiev and B. S. Khodzhiev, *Vysokochist. veshchestva [High-Purity Substances]*, 1993, No. 5, 111 (in Russian).
79. Sh. Sh. Nabiev, I. I. Ostroukhova, L. A. Palkina, and B. S. Khodjiev, *Proc. XI Symp. and School on High Resol. Molec. Spectrosc.* (Moscow—Nizhnii Novgorod, 1993), SPIE Publ., Washington, 1994, **2205**, 261.
80. Sh. Sh. Nabiev, *Preprint IAE* No. 5148/12, Kurchatov Institute of Nuclear Energy, Moscow, 1990, 37 pp. (in Russian).
81. S. M. Melikova, Sh. Sh. Nabiev, and B. A. Fomin, *Proc. XI Symp. and School on High Resol. Molec. Spectrosc.* (Moscow—Nizhnii Novgorod, 1993), SPIE Publ., Washington, 1994, **2205**, 258.
82. Sh. Sh. Nabiev, D. A. Raldugin, V. A. Revin, P. G. Sennikov, and B. S. Khodzhiev, *Preprint IAE* No. 5676/12, Kurchatov Institute of Nuclear Energy, Moscow, 1993, 22 pp. (in Russian).
83. P. G. Sennikov, D. A. Raldugin, and Sh. Sh. Nabiev, *Abstr. XXII Europ. Congr. on Mol. Spectrosc.* (Essen, 1994), GDCh Publ., Essen, 1994, 148.
84. Sh. Sh. Nabiev and B. S. Khodzhiev, *Vysokochist. veshchestva [High-Purity Substances]*, 1994, No. 2, 33 (in Russian).
85. A. V. Mamchenko and Sh. Sh. Nabiev, *Abstr. Intern. Conf. "Actinides-93" (Santa Fe, 1993)*, LALP, Los Alamos, 1993, 18.
86. J. H. Holloway, *Chem. Britain*, 1987, **23**, 658.
87. C. J. Adams and H. Bartlett, *Isr. J. Chem.*, 1978, **17**, 114.
88. K. Leary, D. H. Templeton, A. Zalkin, and N. Bartlett, *Inorg. Chem.*, 1973, **12**, 1726.
89. Sh. Sh. Nabiev, *Vysokochist. veshchestva [High-Purity Substances]*, 1993, No. 5, 138 (in Russian).
90. Sh. Sh. Nabiev, *Proc. Symp. "Molekulyarnoe svetorasseyanie i relaksatsionnye protsessy v zhidkikh sredakh" [Molecular Light Scattering and Relaxation Processes in Liquid Media]*, izd. Samarkandskii Univ., Samarkand, 1993, 11 (in Russian).
91. F. Schreiner, D. W. Osborne, J. G. Malm, and G. N. Mcdonald, *J. Chem. Phys.*, 1969, **51**, 4838.
92. Sh. Sh. Nabiev, *Preprint IAE* No. 5724/12, Kurchatov Institute of Nuclear Energy, Moscow, 1994, 20 pp. (in Russian).
93. Sh. Sh. Nabiev, *Zh. Neorg. Khim.*, 1995, **40**, 2016 [*Russ. J. Inorg. Chem.*, 1995, **40** (Engl. Transl.)].
94. Sh. Sh. Nabiev, *Abstr. Intern. Conf. "Actinides-93" (Santa Fe, 1993)*, LALP, Los Alamos, 1993, 108.
95. G. L. Gusev and A. I. Boldyrev, *Zh. Neorg. Khim.*, 1989, **34**, 1063 [*Russ. J. Inorg. Chem.*, 1989, **34** (Engl. Transl.)].
96. G. M. Bancroft, D. J. Bristow, J. S. Tse, and G. J. Schrobilgen, *Inorg. Chem.*, 1983, **22**, 2673.
97. H. Meinert and S. Rudiger, *Z. Chem.*, 1967, **7**, 239.
98. Sh. Sh. Nabiev and I. I. Ostroukhova, *Preprint IAE* No. 5326/12, Kurchatov Institute of Nuclear Energy, Moscow, 1991, 15 pp. (in Russian).
99. Sh. Sh. Nabiev and I. I. Ostroukhova, *J. Fluor. Chem.*, 1992, **58**, 287.
100. V. D. Klimov, Sh. Sh. Nabiev, A. P. Osipov, A. V. Ryzhkov, V. B. Sokolov, and V. P. Ushakov, *Abstr. VII*

Vsesoyuzn. simp. po khimii neorg. fioridov [*VII All-Union Symp. on the Chemistry of Inorganic Fluorides*] (Polevskoi, 1987), Nauka, Moscow, 1987, 195 (in Russian).
101. Sh. Sh. Nabiev, A. V. Ryvkov, V. B. Sokolov, *Sb. nauchn. trudov IAE* [*Collection of Scientific Works of the Institute of Nuclear Energy*], Moscow, 1990, **1**, 152 (in Russian).
102. B. Desbat and P. Huong, *J. Chem. Phys.*, 1983, **78**, 6377.
103. D. J. Reynolds, *Adv. Inorg. Chem.*, 1973, **7**, 1.
104. K. O. Christe, E. C. Curtis, and R. D. Wilson, *J. Inorg. Nucl. Chem. Suppl., H. H. Hyman Memorial Volume*, Eds. J. J. Katz and I. Sheft, Pergamon Press, Oxford, 1976, 159.
105. B. Zemva and A. Jesih, *J. Fluor. Chem.*, 1984, **24**, 281.
106. B. Druzina and B. Zemva, *J. Fluor. Chem.*, 1988, **39**, 309.
107. Sh. Sh. Nabiev and B. S. Khodzhiev, *Abstr. IX Vsesoyuzn. simp. po khimii neorg. fioridov* [*IX All-Union Symp. on the Chemistry on Inorganic Fluorides*] (Cherepovets, 1990), izd. MKhTI, Moscow, 1990, 239 (in Russian).
108. Sh. Sh. Nabiev, V. V. Klimov, and B. S. Khodzhiev, *Abstr. V Vsesoyuzn. konf. po khimii nizkikh temperatur* [*V All-Union Conf. on the Low-Temperature Chemistry*] (Moscow, 1991), izd. MGU, Moscow, 1991, 99 (in Russian).
109. Sh. Sh. Nabiev and B. S. Khodzhiev, *Preprint IAE* No. 5723/12, Kurchatov Institute of Nuclear Energy, Moscow, 1993, 20 pp. (in Russian).
110. Sh. Sh. Nabiev, V. P. Novikov, V. V. Klimov, T. M. Kuznetsova, and L. D. Shustov, *Zh. Prikl. Spektr.*, 1987, **46**, 493 [*J. Appl. Spectr.*, 1987, **46** (Engl. Transl.)].
111. Sh. Sh. Nabiev, V. V. Klimov, and T. M. Kuznetsova, *Preprint IAE* No. 5723/12, Kurchatov Institute of Nuclear Energy, Moscow, 1988, 13 pp. (in Russian).
112. Sh. Sh. Nabiev and V. V. Klimov, *Zh. Neorg. Khim.*, 1991, **36**, 1254 [*Russ. J. Inorg. Chem.*, 1991, **36** (in Russian)].
113. Sh. Sh. Nabiev, Sc. D. (Physics and Mathematics) Thesis, Russian Scientific Center "Kurchatov Institute", Moscow, 1995, 336 pp. (in Russian).
114. Sh. Sh. Nabiev and L. P. Sukhanov, *Abstr. II Vserossiiskoi nauch. konf. "Fiziko-khimicheskie protsessy pri selektsii atomov i molekul"* [*II All-Russian Scientific Conf. "Physico-chemical Processes in the Selection of Atoms and Molecules"*] (Zvenigorod, 1997), izd. RNTs "Kurchatovskii institut", Moscow, 1997, 27 (in Russian).
115. S. A. Kirillov and Sh. Sh. Nabiev, *Preprint IAE* No. 5474/12, Kurchatov Institute of Nuclear Energy, Moscow, 1992, 11 pp. (in Russian).
116. V. N. Prusakov and V. B. Sokolov, *Atom. Energiya* [*Atomic Energy*], 1971, **31**, 259 (in Russian).
117. C. Coulson, *J. Chem. Phys.*, 1966, **44**, 468.
118. Sh. Sh. Nabiev, *Preprint IAE* No. 5643/12, Kurchatov Institute of Nuclear Energy, Moscow, 1993, 16 pp. (in Russian).
119. Sh. Sh. Nabiev, *Proc. X Europ. Conf. on Dynamics of Molec. Collisions*, Inst. Matem. Fisica Fund. Publ., Salamanca, 1994, 153.
120. Sh. Sh. Nabiev and L. A. Palkina, *J. Fluor. Chem.*, 1991, **54**, 345.
121. Sh. Sh. Nabiev and L. A. Palkina, *Abstr. XXI Europ. Congr. on Molec. Spectrosc.*, Tech. Univ. Publ., Vienna, 1992, E32.

Received October 22, 1997
in revised form December 26, 1997